ISSN 0869-5938, Stratigraphy and Geological Correlation, 2016, Vol. 24, No. 3, pp. 219–241. © Pleiades Publishing, Ltd., 2016.
Original Russian Text © Yu.N. Smirnova, A.A. Sorokin, A.B. Kotov, V.P. Kovach, 2016, published in Stratigrafiya. Geologicheskaya Korrelyatsiya, 2016, Vol. 24, No. 3, pp. 3–26.

Tectonic Conditions of Sedimentation and Source Areas of Upper Proterozoic and Lower Paleozoic Terrigenous Deposits of the Lesser Khingan Terrane of the Central Asian Fold Belt

Yu. N. Smirnova[a], A. A. Sorokin[a], A. B. Kotov[b], and V. P. Kovach[b]

[a] *Institute of Geology and Nature Management, Far Eastern Branch, Russian Academy of Sciences, Blagoveshchensk, Russia*
[b] *Institute of Precambrian Geology and Geochronology, Russian Academy of Sciences, St. Petersburg, Russia*
e-mail: sorokin@ascnet.ru

Received April 28, 2015; in final form, October 5, 2015

Abstract—This work presents the results of geological, geochemical, and Sm-Nd isotopic and geochemical studies of Late Riphean–Cambrian terrigenous rocks of the Khingan Group of the Lesser Khingan Terrane of the Central Asian Fold Belt, as well as the results of U-Pb geochronological (LA-ICP-MS) studies of detrital zircons from these deposits. These deposits are the most ancient in the structure of the terrain. It was found that the deposits of Iginchi and underlying Murandavi formations are attributed to the Late Riphean–Vendian age interval, and the Kimkan sequence, to the Late Cambrian–Early Ordovician. The periods of formation of the Murandavi and Iginchi formations, on one hand, and the Kimkan sequence, on the other hand, are separated by the stage of granitoid magmatism at the turn of the Vendian–Cambrian. Because of this, they cannot be attributed to a unified sedimentary sequence. It is the most probable that the sedimentation of the Iginchi and Murandavi formations and the Kimkan sequence occurred under subduction conditions against the backdrop of magmatic activity.

Keywords: Central Asian Fold Belt, Riphean, Vendian, Cambrian, sedimentary rocks, detrital zircons, depositional settings

DOI: 10.1134/S0869593816030060

INTRODUCTION

The Lesser Khingan (Jiamusi) Terrane (continental block) is a part of the Bureya-Jiamusi Superterrane (Fig. 1) and is one of the largest tectonic structures of the eastern part of the Central Asian Fold Belt (Parfenov et al., 2003; *Geodinamika*... 2006; etc.). Until recently (Selivanov et al., 1995; Dobkin, 2000; *Geodinamika*..., 2006), this terrane was regarded as a classic Early Precambrian sialic block, usually subdivided into the Early Precambrian basement (metamorphic rocks of the Amur Group; the Russian part of the block) and Upper Proterozoic (Upper Riphean)–Cambrian cover (terrigenous–carbonate deposits of the Khingan Group).

However, owing to complex geological, geochronological, and isotope-geochemical studies in recent years, it was established that the conditionally Early Precambrian metamorphic series comprise sedimentary and volcanic rocks of different ages, including Early Precambrian (Wilde et al., 2000, 2003; Kotov et al., 2009a, 2009b; Salnikova et al., 2013; etc.). Accordingly, the age and tectonic conditions of sedimentation of terrigenous–carbonate deposits of the Khingan Group, which are likely one of the most ancient formations in the structure of the Lesser Khingan Terrane, are debatable issues. Moreover, the interest in the latter is fueled by the fact that the reconstruction of Late and Early Paleozoic processes is a key to understanding the history of the formation of orogenic structures in Central Asia (Mossakovskii et al., 1993; Didenko et al., 1994; Parfenov et al., 2003; etc.).

In this regard, we have carried out comprehensive geological, geochemical, and geochronological isotope-geochemical studies of rocks of the Khingan Group to clarify their age and determine the conditions of their accumulation.

BRIEF DESCRIPTION OF THE LESSER KHINGAN TERRANE

As noted above, the metamorphic series of the Amur Group within the Russian part of the terrain in the correlation schemes developed for geological complexes of the Lesser Khingan Terrane (*Resheniya*..., 1994; Selivanov et al., 1995; Dobkin, 2000; *Geodinamika*..., 2006; etc.) are attributed to the most ancient formations.

However, as a result of complex geological, U-Pb geochronological, and Sm-Nd isotopic and geochemical studies, it has been recently established that the

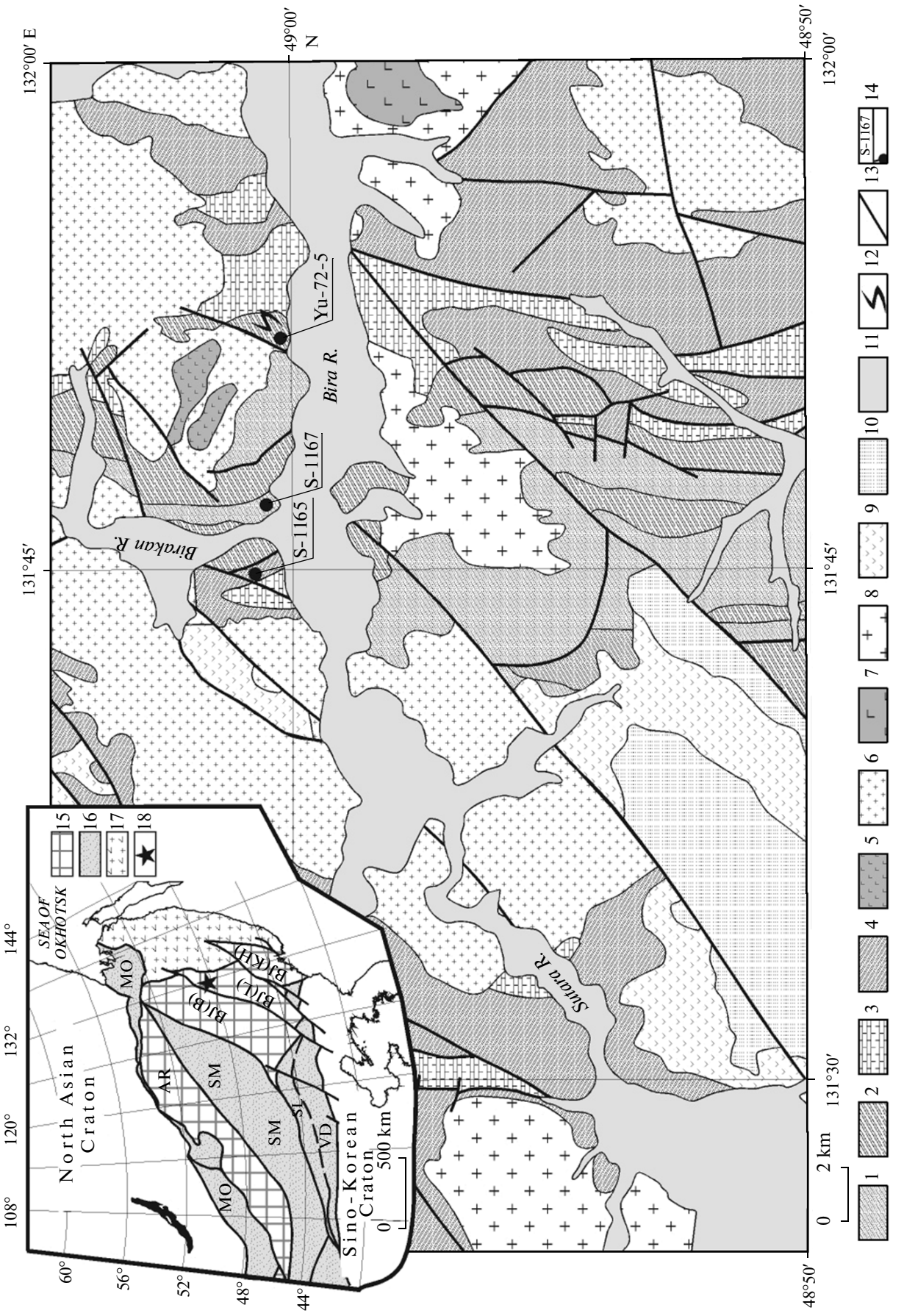
132°00′ E
49°00′ N
48°50′
132°00′
131°45′
131°30′
Yu-72-5
S-1167
S-1165
Bira R.
Birakan R.
Siniara R.
0 2 km
1
2
3
4
5
6
7
8
9
10
11
12
13 S-1167
14
15
16
17
18
SEA OF OKHOTSK
North Asian Craton
Sino-Korean Craton
MO
AR
SM
SL
VD
BJK
0 500 km
108°
120°
132°
144°
60°
56°
52°
48°
44°

protoliths of metamorphic rocks of this group have a younger age, but not Early Precambrian as previously thought. In particular, the minimum age of detrital zircons from metasedimentary rocks of the Uril Formation of the Amur Group is about 240 Ma, which to a first approximation corresponds to the lower age boundary of the formation of their protoliths. The upper age boundary (220–210 Ma) of accumulation of protoliths of metasedimentary rocks of this formation is constrained by the age of superimposed structural and metamorphic transformations (Salnikova et al., 2013). At the same time, the Nd model age of metasedimentary rocks of the Tulovchikha Formation of the Amur Group is about 1.7 Ga; the age of gabbro of the Amur Complex intruding metasedimentary rocks is 486 ± 18 Ma (Kotov et al., 2009a, 2009b). In other words, the age of this formation is in the range of 1.7–0.5 Ga. All this indicates that sedimentary and volcanic rocks of different ages, but not Early Precambrian, are "combined" in the sequence of the Amur Group.

The terrigenous–carbonate deposits of the Khingan Group (Iginchi, Murandavi, and Londoko formations, Kimkan sequence) are attributed to the Upper Precambrian (Upper Riphean)–Cambrian stratigraphic level in the correlation schemes of geological complexes available (*Resheniya*..., 1994; Selivanov et al., 1995; Dobkin, 2000; *Geodinamika*..., 2006; etc.) Being considered to be the most ancient structures in the structure of the Lesser Khingan Terrane, these formations attract special attention.

It is known that deposits of the Khingan Group are intruded by Early Paleozoic granitoids of the Birobidzhan and Bira complexes (Martynyuk et al., 1990; Selivanov et al., 1995; Dobkin, 2000; *Geodinamika*..., 2006), the age datings of which are in the range of 480–461 Ma (Sorokin et al., 2010a, 2011), and subalkaline gabbroids of the Ust'-Birakan massif (429 ± 1 Ma; Buchko et al., 2012). In recent years, Cambrian granitoids with age datings in the range of 540–490 Ma have been identified the structure of the Lesser Khingan Terrane (Wu et al., 2011; Bi et al., 2014; Yang et al., 2014; Sorokin et al. (in press)). In addition, the manifestation of high-pressure metamorphism (~500 Ma; Wilde et al., 2000, 2003), indicating that the terrain had a complex history of development in the Early Paleozoic, was found.

According to the current ideas (*Resheniya*..., 1994; Selivanov et al., 1995; Dobkin, 2000; *Geodinamika*..., 2006; etc.), Late Paleozoic magmatic formations are represented by Middle–Late Carbonaceous multiphase gabbro-diorite-granodiorite-granite intrusions of the Tyrma–Bureya complex and Permo-Triassic subalkaline leucogranites, granites, and syenites of the Kharinskii complex. There are no reliable geochronological data for these formations within the Lesser Khingan Terrane, except for gabbroids of the Kimkan sequence (257 ± 1 Ma; Buchko et al., 2011, 2013). At the same time, petrotypical massifs of the Tyrma-Bureya and Kharinskii complexes, which crop out within the Bureya (Turan) Terrane have Late Triassic–Early Jurassic age (Sorokin et al., 2010b; Sorokin and Kudryashov, 2013).

Finally, the youngest formations superimposed on this complex structural collage are represented by vast fields of Late Mesozoic volcanics and intrusions of the Khingan–Okhotsk Belt (*Geodinamika*..., 2006).

This work is aimed at studying terrigenous rocks of the Iginchi and Murandavi formations and Kimkan sequence of the Upper Riphean–Cambrian Khingan Group.

OBJECTS OF STUDY

In this work, we do not consider deposits of the Khingan Group in detail since they have already been described in the literature (Selivanov et al., 1995; Dobkin, 2000; *Geodinamika*..., 2006; Smirnova and Sorokin (in press)).

In the framework of developed explanatory notes to state geological maps of the third generation, the following sequence of sedimentary formations is proposed (from top to bottom): Iginchi (more than –1000 m), Murandavi (1300–2500 m), Londoko (1000 m) formations, Kimkan sequence (900–2000 m) (Selivanov et al., 1995; Dobkin, 2000; *Geodinamika*..., 2006).

The Iginchi Formation is composed of interbedded sandstones and siltstones and, to a lesser extent, quartz-sericite schists and phyllites. The Murandavi Formation is composed of calcareous dolomites, siltstones, and siliceous-clayey shales with intercalations of hematite and magnetite-hematite ores, limestones, sandstones, and rarely magnesites. The Londoko For-

Fig. 1. Geological scheme of the northern part of the Lesser Khingan terrane of the eastern part of the Central Asian Fold Belt (modified after (Dobkin, 2000)). (1) Conditionally Upper Riphean siltstones, sandstones, and mudstones of the Iginchi Formation; (2) conditionally Vendian-Lower Cambrian sandstones, limestones, and siltstones of the Murandavi Formation; (3) Lower Cambrian limestones, dolomites, clayey shales, and sandstones of the Londoko Formation; (4) Lower Cambrian sandstones and siltstones of the Kimkan sequence; (5) Early Paleozoic gabbro and diorites; (6) Early Paleozoic granites, granodiorites, leucogranites, quartz monzonites, and granosyenites; (7) conditionally Late Paleozoic gabbro and diorites; (8) conditionally Late Paleozoic granites, granodiorites, and quartz diorites; (9) Early Cretaceous andesites, andesitic basalts, Early to Late Cretaceous rhyolites and their lavas, lava breccias, and tuffs; (10) Upper Cretaceous sandstones, conglomerates, and siltstones; (11) Cenozoic loose deposits; (12) conventional body of gneissic granites (536 ± 6 Ma); (13) faults; (14) sampling sites for U-Pb geochronology (LA-ICP-MS) and their numbers. In the map inset: the tectonic scheme showing positions of the sites of study in the structure of the eastern part of the Central Asian Fold Belt (after (Parfenov et al., 2003)). (1) Continental massifs (AR—Argun, BJ(B)—Bureya, BJ(L)—Lesser Khingan, BJ(KH)—Khanka); (16) Paleozoic–Early Mesozoic fold belts (SM—South Mongolian, SL—Solonker, VD—Vundurmiao); (17) Late Jurassic–Early Cretaceous orogenic belts; (18) area of study.

Eon	Erathem	System	Division	Index	Lithology	Thickness, m	Description of subdivisions
	Paleozoic	Cambrian	Lower	$\in_1 km_2$		>855	Kimkan sequence (upper subsequence). Sandstone, siltstone, clayey shales (occasionally carbonaceous), intercalations of phtanites and limestones rare rhyolite and basalt tuffs
				$\in_1 km_1$		900–1070	Kimkan sequence (lower subsequence). Clayey, siliceous-clayey, and carbonaceous shales, phtanites, siltstones, sandstones, limestones, dolomites, jasper-like siliceous rocks with intercalations of hematite and magnetite ores and rhyolites.
				$\in_1 ln$		1000	Londoko Formation. Limestones, occasionally dolomitic, rare dolomites with intercalations of clayey and carbonaceous siliceous-clayey shales, limestone and phosphorite-limestone breccias, phtanites
				$V\text{-}\in_1 mr_2$		695–900	Murandavi Formation (upper subformation). Dolomites, carbonaceous dolomites, siltstones, siliceous-clayey and clayey shales, jasper-like siliceous rocks with intercalations of hematite and magnetite-hematite ores, dolomite and phosphorite-dolomite breccias, limestones, sandstones, phtanites, spongolites, marls, rare magnesites, rhyolite tuffs
Upper Proterozoic		Vendian		Vmr_1		600–750	Murandavi Formation (lower subformation). Dolomites, magnesites, rare beds of phtanites, clayey shales, rhyolites
	Upper Riphean			$R_3 ig$		>1000	Iginchi Formation. Sandstone, siltstone, clayey shale, rare dolomite intercalations in the upper part

Fig. 2. Generalized stratigraphic column of terrigenous rocks of the Khingan Group of the Lesser Khingan Terrane (modified after (Dobkin, 2000)).

mation is represented by limestones alternating with carbonaceous and clayey shales. The Kimkan sequence is predominantly made of clayey and siliceous-clayey, as well as carbonaceous shales, phtanites, siltstones, sandstones, and limestones (Fig. 2).

On the basis of findings of Lower Atdabanian microphytolites, sponges, and brachiopods, the upper age boundary of deposits of the Khingan Group is considered to be the Lower Cambrian; the lower age boundary is considered conditionally to be the Upper Riphean (Selivanov et al., 1995; Dobkin, 2000; *Geodinamika*.., 2006).

It was noted above that the deposits of this group are intruded by Early Paleozoic intrusions with the age of 480–429 Ma (Sorokin et al., 2010a, 2011; Buchko et al., 2012). In addition, according to new data (Sorokin et al. (in press)), terrigenous sediments of the Murandavi Formation of the Khingan Group are intruded by dike bodies of hornblende gneissogranites with the age of 535 ± 6 Ma. These data indicate that the introduction of these dikes was at the turn of the Vendian–Cambrian and the accumulation of terigenous rocks of the Khingan Group (Murandavi and underlying Iginchi formations) occurred in the Late Proterozoic.

In general, the presence of Cambrian granitoids in the structure of the Lesser Khingan Terrain (Wu et al., 2011; Bi et al., 2014; Yang et al., 2014; Sorokin et al. (in press)) and the manifestation of the granulite metamorphism stage (~500 Ma; Wilde et al., 2000, 2003) contradict the idea of the continuous evolution of the Khingan Group lasting from the Late Riphean to Cambrian (*Resheniya*..., 1994; Selivanov et al., 1995; Dobkin, 2000; *Geodinamika*..., 2006) (Fig. 2).

RESEARCH METHODS

Studies of the chemical composition of rocks were performed using the X-ray fluorescence (the major components, Zr) at the Institute of Geology and Nature Management, Far Eastern Branch, Russian Academy of Sciences (Blagoveshchensk) and ICP-MS (Li, Rb, Sr, Ba, REE, Y, Th, U, Nb, Ta, Zn, Co, Ni, Sc, V, Cr) methods at the Institute of Tectonics and Geophysics, Far Eastern Branch, Russian Academy of Sciences (Khabarovsk). Homogenization of powder samples for the X-ray fluorescence analysis was performed by fusing of them with a mixture of lithium metaborate and tetraborate in a muffle furnace at 1050–1100°C. The measurements were performed using a Pioneer 4S X-ray spectrometer. The intensity of analytical lines was corrected for background absorbance and secondary fluorescence. For the ICP-MS analysis, samples were decomposed with acid. Measurements were made using an Elan 6100 DRC in standard mode. The device sensitivity mass calibration was performed using standard solutions comprising all elements in the samples being analyzed. The relative error in determining the contents of major and minor elements is 5–10%.

The concentrations and isotopic compositions of Sm and Nd were determined at the Institute of Precambrian Geology and Geochronology, Russian

Academy of Sciences (St. Petersburg). Samples of 100 mg pounded into powder and spiked with a mixed ^{149}Sm-^{150}Nd spike were decomposed in Teflon vessels in a mixture of HCI + HF + HNO_3 at a temperature of 110°C. The completeness of decomposition was checked under a binocular microscope. The Nd and Sm isotopic compositions were measured on a TRITON TI multicollector mass spectrometer in static mode. The measured $^{143}Nd/^{144}Nd$ ratio was normalized to the ratio $^{146}Nd/^{144}Nd = 0.7219$ and then to the ratio $^{143}Nd/^{144}Nd = 0.512115$ in the Nd standard JNdi-1. The weighted average $^{143}Nd/^{144}Nd$ in the Nd standard JNdi-1 for the measurement period was 0.512108 ± 8 ($n = 7$). The laboratory blanks were 0.03–0.2 ng for Sm and 0.1–0.5 ng for Nd. The accuracy of determining the Sm and Nd isotope concentrations was ±0.5%; the accuracy of determining the $^{147}Sm/^{144}Nd$ and $^{143}Nd/^{144}Nd$ isotope ratios was ±0.5 and ±0.005%, respectively. In order to calculate $\varepsilon_{Nd}(t)$ values and model ages $t_{Nd(DM)}$, the modern CHUR values ($^{143}Nd/^{144}Nd = 0.512638$, $^{147}Sm/^{144}Nd = 0.1967$) after (Jacobsen and Wasserburg, 1984) and DM values ($^{143}Nd/^{144}Nd = 0.513151$, $^{147}Sm/^{144}Nd = 0.2136$) after (Goldstein and Jacobsen, 1988) were used.

Zircon grains were extracted using heavy liquids in the mineralogical laboratory of the Institute of Geology and Nature Management (Blagoveshchensk). The U-Pb geochronological study of detrital zircons (about 100 grains from each sample) was performed in the GeoAnalytical Lab of Washington State University (USA) using an ELEMENT 2 ICP-MS mass spectrometer equipped with a New Wave YAG 213 laser ablation system with a preliminary study of the internal structure of zircon grains on CL images. The diameter of the crater did not exceed 20 μm. Calibration was performed using the standards FC (Duluth complex, 1099.0 ± 0.6 Ma (Paces and Miller, 1993)), MD (Mt. Dromedary, 99.12 ± 0.14 Ma (Renne et al., 1998)), R3 (Braintree complex, 418.9 ± 0.4 Ma (Black et al., 2004)), and T2 (Temora 2, 416.78 ± 0.33 Ma (Black et al., 2004)). Experimental data were processed using ISOPLOT software (Ludwig, 1999). The $^{206}Pb/^{238}U$ and $^{207}Pb/^{206}Pb$ ratios were continuously monitored during the measurement in order to avoid abnormal values related to the measurement of nonhomogeneous sites with varying age zoning and inclusions. The data interpretation was performed according to the recommendations given in (Whitehouse et al., 1999; Gehrels, 2011). In particular, only those age datings were taken into consideration whose discordance did not exceed 10%. For zircons whose ages were more ancient than 1.0 Ga, the $^{207}Pb/^{206}Pb$ ages were used; for younger zircons, the $^{206}Pb/^{238}U$ ages were used. All age errors in the text and figures are given at the level ±2σ.

MAJOR PETROGRAPHIC AND GEOCHEMICAL FEATURES OF ROCKS

The Iginchi Formation is dominated by massive silty sandstones and small-, medium-, and coarse-grained dark, light, and greenish gray sandstones. They are composed of angular, semiangular, and rarely subrounded fragments of quartz (40–60%), feldspar (15–20%), biotite flakes (10–15%), muscovite (5–15%), and single grains of epidote (up to 5%). The accessory minerals are dominated by zircon, sphene, leucoxene, apatite, and ore minerals. The texture is blastoaleuropsammitic and blastopsammitic. Mica-siliceous cement is basal, contact, and porous.

The terrigenous rocks of the Murandavi Formation are dominated by small- and medium-grained massive light gray, yellowish gray, and dark gray sandstones. The clastic material is represented by quartz (30–65%), feldspar (5–30%), biotite flakes (10–15%), and muscovite (5–15%); volcanic material and carbonates occur as single fragments. Accessory minerals are dominated by zircon, apatite, garnet, sphene, and ore minerals. The texture is blastopsammitic. The micaceous–siliceous cement is contact.

The Kimkan sequence is dominated by massive and schistose dark gray and greenish gray silty sandstones. They are composed of slightly angular and subrounded fragments of quartz (40–50%), feldspar (15–25%), biotite flakes (10–15%), and muscovite (5–10%), as well as fragments of volcanic rocks and quartzite. Such minerals as zircon, sphene, leucoxene, and ore minerals dominate among accessory minerals. The texture is blastoaleuropsammitic. The cement is basal, rarely contact micaceous–siliceous and hydromica–ferruginous.

The mineralogical composition of polymictic terrigenous rocks of the Khingan Group is a reason that these rocks are enriched in Na_2O, Al_2O_3, $Fe_2O_3^*$ with respect to SiO_2 (Table 1). According to these peculiarities, their figurative points on the classification diagrams are mainly located in the fields of greywacke, sub-greywacke (Figs. 3a–3c), and polymictic sandstones (Fig. 3d).

One of the main methods of studying the sedimentary formations is the calculation of petrochemical modules and indexes. By analyzing these parameters, we can clarify the petrochemical classification of rocks and reconstruct the physical and chemical conditions of sedimentation. As follows from Table 2, where some of the most commonly used petrochemical parameters are given, the values of geochemical modules and indexes for terrigenous rocks of the Khingan Group vary within narrow ranges. There is a slight tendency for the following modules to increase: $AM = Al_2O_3/SiO_2$ (Ketris, 1976), $TM = TiO_2/Al_2O_3$ (Migdisov, 1960), the total normalized alkalinity (feldspar indicator) $SPM = (Na_2O + K_2O)/Al_2O_3$ (Yudovich, 1981) in sandstones and silty sandstones of the Kimkan sequence compared

Table 1. Chemical compositions of representative samples of Upper Proterozoic and Lower Paleozoic terrigenous deposits of the Khingan Group of the Lesser Khingan terrane

Components	Iginchi Formation													
	Silty sandstones											Sandstone		
	S-1167	S-1167-2	S-1167-3	S-1167-6	S-1168	S-1168-1	S-1168-2	S-1168-3	S-1168-4	S-1168-6	S-1168-7	S-1169	S-1169-1	S-1169-2
SiO_2	73.70	65.28	72.10	74.27	76.43	71.44	71.31	73.41	73.08	75.64	74.63	75.53	67.87	69.94
TiO_2	0.74	0.90	0.77	0.59	0.62	0.95	0.78	0.76	0.82	0.66	0.67	0.62	0.93	0.94
Al_2O_3	11.27	15.70	10.92	9.83	9.93	13.77	11.72	11.45	11.36	10.16	10.79	9.29	12.95	11.57
$Fe_2O_3^*$	7.12	7.23	8.15	7.23	6.82	6.23	6.84	7.67	7.76	6.93	6.92	7.39	6.97	6.84
MnO	0.05	0.05	0.06	0.04	0.06	0.06	0.07	0.07	0.06	0.06	0.06	0.06	0.09	0.10
MgO	1.43	1.69	1.67	1.66	1.44	1.21	1.91	1.41	1.36	1.29	1.35	1.47	1.99	1.92
CaO	0.80	0.85	0.86	0.91	0.84	0.72	1.85	0.82	0.73	0.86	1.06	0.96	2.14	2.51
Na_2O	0.78	0.81	0.92	1.37	0.59	0.64	1.40	0.82	0.86	0.82	1.08	1.05	3.01	2.02
K_2O	2.50	3.83	2.70	2.01	2.14	2.85	2.27	2.40	2.48	2.04	2.08	2.26	2.61	2.31
P_2O_5	0.12	0.12	0.12	0.13	0.11	0.10	0.08	0.12	0.10	0.09	0.10	0.10	0.18	0.17
p.p.p.	1.24	2.93	1.39	1.72	0.85	1.71	1.49	0.90	1.16	1.19	1.06	1.04	1.03	1.35
Total	99.75	99.39	99.66	99.76	99.83	99.68	99.72	99.83	99.77	99.74	99.80	99.77	99.77	99.67
Li	25	29	29	23	46	35	50	35	39	37	42	65	43	43
Rb	128	157	125	85	135	123	160	135	138	114	97	135	98	96
Sr	72	85	75	80	76	86	204	92	107	117	127	89	116	145
Ba	567	860	643	455	374	615	374	454	472	426	460	370	509	405
La	23.84	23.20	20.20	25.54	25.79	35.61	29.57	29.06	27.40	28.88	33.62	36.92	30.30	30.59
Ce	50.44	47.62	42.15	53.89	54.53	90.51	62.66	62.63	59.36	61.40	86.25	93.79	63.41	63.30
Pr	5.79	5.50	4.90	6.28	6.25	9.05	7.22	7.24	6.80	7.05	8.38	9.06	7.64	7.66
Nd	22.65	21.50	19.12	24.28	24.44	35.13	28.44	28.70	26.66	27.70	32.48	35.61	31.10	29.92
Sm	4.20	4.20	3.68	4.54	4.81	6.67	5.38	5.46	5.01	5.13	6.16	6.39	6.15	5.75
Eu	0.79	0.91	0.66	0.85	0.86	1.17	1.29	0.96	0.91	0.91	1.10	1.13	1.32	1.20
Gd	4.06	3.88	3.40	4.36	4.54	6.16	4.83	5.08	4.64	4.52	5.65	5.85	5.99	5.63
Tb	0.40	0.41	0.36	0.47	0.46	0.61	0.48	0.50	0.45	0.44	0.56	0.59	0.66	0.62
Dy	1.76	1.89	1.59	2.06	1.86	2.38	1.88	1.97	1.75	1.74	2.31	2.38	2.93	2.87
Ho	0.29	0.33	0.27	0.32	0.27	0.34	0.28	0.28	0.23	0.25	0.33	0.35	0.44	0.46
Er	0.84	0.97	0.77	0.89	0.73	0.88	0.76	0.71	0.60	0.70	0.88	0.90	1.11	1.27
Tm	0.11	0.15	0.12	0.12	0.09	0.10	0.10	0.08	0.06	0.08	0.11	0.10	0.13	0.16
Yb	0.86	1.04	0.79	0.85	0.65	0.76	0.75	0.57	0.47	0.61	0.77	0.66	0.85	1.13
Lu	0.14	0.18	0.13	0.14	0.10	0.12	0.12	0.09	0.07	0.10	0.13	0.10	0.12	0.18
Y	27	33	29	25	28	36	28	30	30	25	29	25	31	29
Th	9.01	8.48	10.10	9.91	9.32	10.89	9.35	9.98	9.58	9.52	12.09	15.99	8.80	8.62
U	1.43	2.10	1.60	1.57	1.82	2.80	1.98	2.08	2.02	2.00	2.32	2.15	2.23	1.98
Zr	212	194	258	194	209	234	213	241	236	209	240	265	189	217
Nb	8.00	10.00	7.00	7.00	8.00	11.00	9.00	9.00	10.00	8.00	8.00	7.00	9.00	9.00
Ta	0.82	0.75	0.79	0.57	0.70	1.05	0.85	0.86	0.91	0.74	0.85	0.76	0.98	0.85
Zn	76	84	73	30	70	69	68	60	61	75	75	66	70	56
Co	14	20	17	20	17	15	12	18	16	11	18	13	21	14
Ni	25	39	25	27	26	23	15	24	16	12	31	17	37	26
Sc	10.45	15.75	10.85	8.84	9.27	13.18	12.30	10.84	10.82	11.30	11.22	9.42	14.30	11.81
V	72	133	77	69	67	105	88	85	82	71	70	65	95	81
Cr	110	97	100	139	98	119	154	111	94	132	138	191	140	310

Table 1. (Contd.)

Components	Murandavi Formation										
	Sandstone										
	Yu-72	Yu-72-1	Yu-72-2	Yu-72-3	Yu-72-4	Yu-72-5	Yu-72-6	Yu-72-7	S-1170-1	S-1170-2	S-1170-3
SiO_2	70.30	69.09	72.82	71.77	69.15	70.62	74.91	68.90	71.11	69.71	65.36
TiO_2	0.93	1.01	0.82	0.70	1.00	0.92	0.70	1.05	0.91	0.85	1.03
Al_2O_3	11.87	13.09	10.69	11.48	12.45	11.70	10.80	12.43	12.01	12.81	13.68
$Fe_2O_3^*$	6.42	6.77	6.12	6.14	6.67	6.47	6.13	6.97	6.91	6.93	8.57
MnO	0.08	0.07	0.08	0.08	0.07	0.08	0.08	0.08	0.08	0.07	0.09
MgO	1.84	2.00	1.51	1.26	2.11	1.72	1.30	1.87	2.00	1.76	2.26
CaO	1.64	0.91	2.20	1.87	1.42	1.64	2.81	1.87	1.90	2.2	2.09
Na_2O	2.30	1.28	2.05	1.80	1.62	2.31	0.57	2.07	1.70	1.72	1.52
K_2O	2.93	2.12	4.02	1.85	1.40	3.13	2.03	1.42	2.34	2.72	2.48
P_2O_5	0.15	0.15	0.15	0.16	0.11	0.14	0.15	0.15	0.14	0.20	0.15
p.p.p.	3.85	0.89	1.10	0.54	2.18	1.38	0.88	1.29	0.74	0.82	2.26
Total	100.15	99.83	98.54	99.49	98.84	98.79	99.14	98.52	99.84	99.79	99.49
Li	28	40	29	20	27	25	18	20	42	31	66
Rb	68	132	91	54	104	73	66	79	96	105	128
Sr	147	132	130	149	123	144	170	147	141	143	120
Ba	482	849	232	221	552	436	380	454	637	614	369
La	36.82	46.10	31.54	31.81	34.73	29.89	23.64	29.19	30.26	26.86	30.14
Ce	67.43	105.18	75.92	56.72	80.26	57.23	48.80	62.77	64	57.06	64.33
Pr	7.36	10.10	8.32	6.73	9.18	7.66	7.19	9.15	7.55	6.67	7.57
Nd	31.37	34.51	30.52	28.71	33.50	31.94	28.27	35.09	30.28	26.92	30.42
Sm	7.25	7.05	5.48	6.37	5.99	6.66	5.53	6.33	5.90	5.32	5.89
Eu	1.94	1.96	1.06	1.74	1.34	1.51	1.22	1.25	1.28	1.35	1.16
Gd	7.56	9.45	6.67	6.27	7.00	5.64	4.89	5.73	5.78	5.14	5.73
Tb	0.82	0.92	0.83	0.75	0.76	0.75	0.81	0.88	0.63	0.59	0.64
Dy	4.87	3.22	3.78	4.91	2.88	4.28	5.06	4.57	2.68	2.7	2.73
Ho	1.04	0.56	0.72	1.06	0.43	0.85	0.97	0.80	0.37	0.4	0.38
Er	3.12	1.73	2.41	3.00	1.23	2.13	2.41	2.11	0.84	0.95	0.89
Tm	0.37	0.19	0.37	0.37	0.14	0.28	0.37	0.33	0.09	0.1	0.09
Yb	2.31	1.10	2.63	2.38	0.81	1.90	2.49	2.28	0.49	0.62	0.53
Lu	0.35	0.12	0.36	0.36	0.10	0.31	0.40	0.36	0.07	0.08	0.08
Y	31	36	31	27	36	31	30	32	26	37	31
Th	10.02	9.51	9.97	9.42	9.66	9.71	8.88	10.22	8.99	7.3	8.87
U	1.53	2.01	1.68	1.86	1.54	1.76	1.67	1.58	1.68	1.79	1.53
Zr	195	225	221	170	231	204	218	272	197	174	214
Nb	12	13	14	11	14	12	11	14	9	10	11
Ta	0.82	0.94	0.70	0.77	0.61	0.80	0.59	0.50	0.80	0.79	0.88
Zn	92	107	78	86	60	96	76	112	84	72	78
Co	15	16	15	14	15	15	15	16	14	14	18
Ni	24	37	25	23	32	24	27	27	34	35	53
Sc	11.24	12.66	9.19	9.56	10.67	11.18	8.79	10.94	13.54	16.41	19.4
V	94	106	69	79	83	90	66	72	89	81	116
Cr	116	152	104	156	141	112	92	120	221	214	230

Table 1. (Contd.)

Components	Kimkan sequence								
	Silty sandstones								
	S-1165	S-1165-1	S-1165-2	S-1165-3	S-1165-4	S-1165-5	S-1165-6	S-1165-7	S-1165-8
SiO_2	72.84	68.89	64.32	66.31	63.01	68.70	68.52	69.79	71.16
TiO_2	0.45	0.61	0.70	0.65	0.72	0.48	0.48	0.56	0.52
Al_2O_3	12.63	13.32	14.63	14.00	14.83	14.09	14.31	13.55	13.29
$Fe_2O_3^*$	3.24	4.84	6.86	6.47	7.11	4.64	4.29	4.53	4.06
MnO	0.08	0.07	0.12	0.11	0.08	0.05	0.06	0.07	0.07
MgO	1.38	2.02	2.53	2.42	2.77	1.77	2.02	1.97	1.76
CaO	2.76	2.94	2.88	3.44	2.33	2.33	3.25	3.03	3.17
Na_2O	2.50	2.11	1.99	2.14	2.13	2.99	1.95	2.16	2.29
K_2O	2.19	3.04	3.06	2.56	4.94	3.53	3.54	2.94	2.19
P_2O_5	0.09	0.13	0.15	0.14	0.15	0.09	0.09	0.11	0.11
p.p.p.	1.46	1.64	2.19	1.43	1.54	1.07	1.21	1.08	1.09
Total	99.62	99.61	99.44	99.67	99.59	99.75	99.73	99.78	99.71
Li	29	40	52	44	52	40	35	33	30
Rb	116	151	170	155	233	162	182	164	132
Sr	209	195	164	165	142	190	176	179	182
Ba	1130	1238	1353	1158	1390	1428	1602	1361	1178
La	45.80	46.97	28.32	29.21	24.13	41.68	27.07	31.84	31.43
Ce	109.64	90.94	77.17	56.51	53.04	98.64	75.53	98.00	89.83
Pr	10.96	11.16	7.34	7.46	6.10	10.30	6.77	7.98	7.70
Nd	40.82	41.86	28.28	28.12	23.75	39.11	25.58	30.04	29.14
Sm	7.89	8.01	6.14	5.67	5.09	7.72	5.37	6.00	5.69
Eu	0.89	1.08	0.95	0.88	0.81	0.98	0.61	0.81	0.75
Gd	8.21	8.24	6.82	5.82	5.36	7.92	5.77	6.38	5.93
Tb	1.09	1.15	1.00	0.81	0.71	1.02	0.80	0.85	0.76
Dy	5.92	6.51	5.80	4.61	3.84	5.32	4.83	4.86	4.28
Ho	1.17	1.29	1.16	0.92	0.73	0.96	0.96	0.94	0.83
Er	3.35	3.88	3.46	2.79	2.14	2.71	2.96	2.81	2.46
Tm	0.46	0.56	0.50	0.43	0.31	0.36	0.45	0.40	0.35
Yb	2.92	3.70	3.43	3.02	2.14	2.40	3.02	2.74	2.36
Lu	0.42	0.54	0.48	0.44	0.34	0.36	0.44	0.41	0.36
Y	36	35	35	23	42	41	25	34	27
Th	26.84	22.16	20.16	21.59	15.62	25.53	28.42	22.17	22.60
U	4.56	7.14	3.24	3.23	3.45	4.68	7.18	5.96	5.29
Zr	187	188	175	179	147	183	193	184	183
Nb	8.00	9.00	9.00	9.00	9.00	10.00	8.00	9.00	8.00
Ta	1.06	1.02	1.12	1.13	1.04	1.29	1.17	1.06	0.98
Zn	77	97	115	100	108	90	93	88	82
Co	7	12	17	15	19	9	8	12	11
Ni	19	22	33	28	32	17	21	24	25
Sc	6.50	8.94	12.09	10.73	13.00	7.83	8.23	9.88	8.37
V	42	62	94	81	121	49	52	72	58
Cr	91	98	94	122	88	84	84	107	102

Oxides are given in wt %; elements are given in ppm. $Fe_2O_3^*$ is total iron.

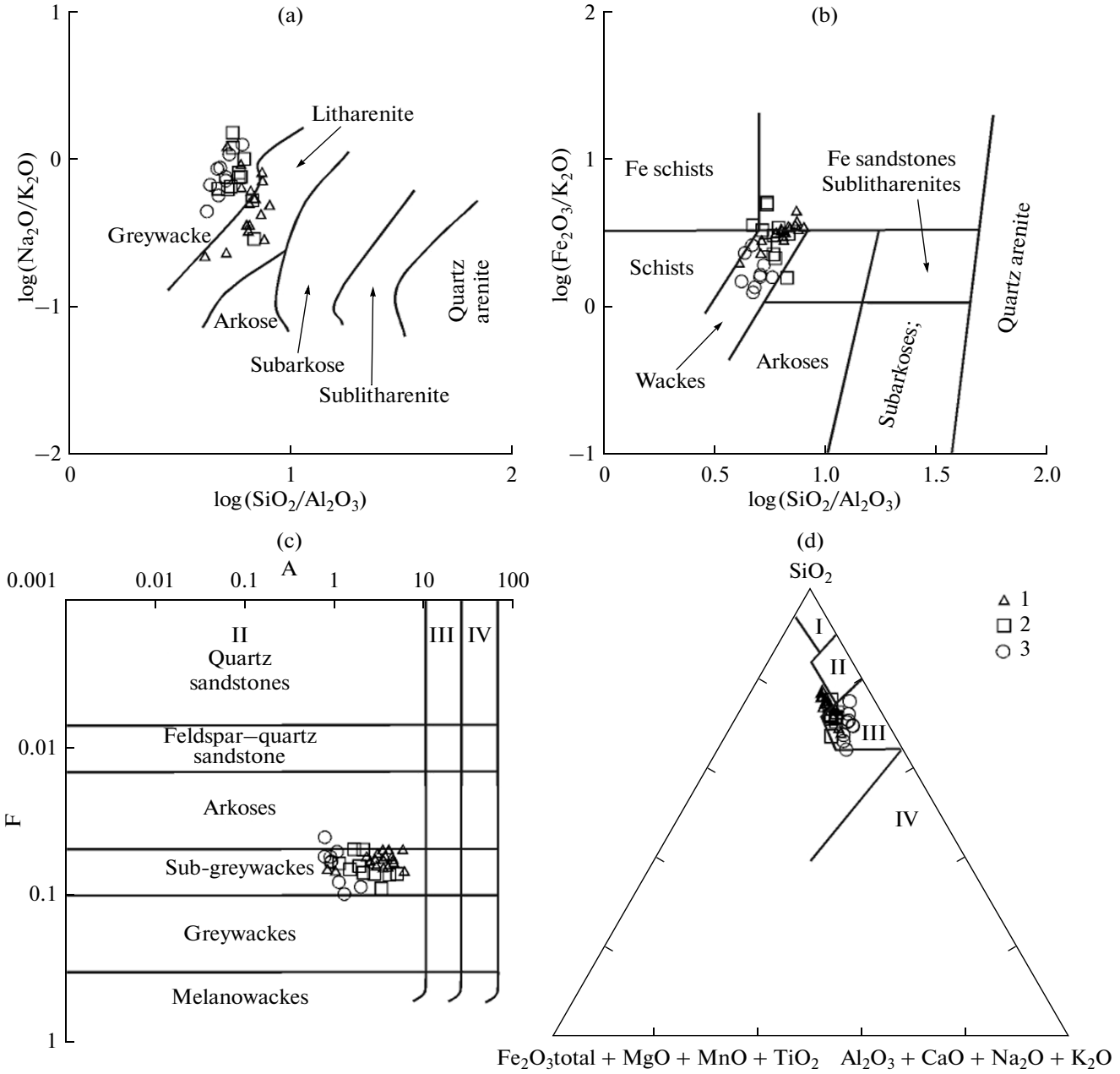

Fig. 3. Set of diagrams compiled for terrigenous rocks of the Khingan Group of the Lesser Khingan Terrane: (a) $\log(SiO_2/Al_2O_3)$–$\log(Na_2O/K_2O)$ (Pettijohn et al., 1972), (b) $\log(SiO_2/Al_2O_3)$–$\log(Fe_2O_3/K_2O)$ (Herron, 1988); (c) A–F (Predovskii, 1980), (d) $(Fe_2O_3total + MgO + MnO + TiO_2)$–$SiO_2$–$(Al_2O_3 + CaO + Na_2O + K_2O)$ (Kossovskaya and Tuchkova, 1988). Legend: (1–3) terrigenous rocks of Iginchi (1), Murandavi (2), and Kimkan (3) formations. Fig. 3c: $A = Al_2O_3$–$(K_2O + Na_2O + CaO)$; $F = (Fe_2O_3 + FeO + MgO)/Si_2O$ (wt %). The fields of low-clay (II), clayey (III), and high-clay (IV) sandy rocks are shown. Fig. 3d: the fields of quartz (I), oligomictic (II), polymictic (III), and volcanoclastic (IV) sandstones are shown.

with sandstones of the Iginchi and Murandavi formations, which is likely associated with an increase in a number of clay minerals in the Kimkan sequence. According to the hydrolysate module $HM = (Al_2O_3 + TiO_2 + Fe_2O_3 + FeO + MnO)/SiO_2 = 0.22–0.46$ (Yudovich et al., 1977) and femic module $FM = (Fe_2O_3 + FeO + MgO)/SiO_2 = 0.06–0.17$ (Yudovich, 1981), terrigenous rocks of the Khingan Group correspond to greywacke and mesomictic and polymictic quartz sandstones and siltstones. Wide variations in the values of the chemical indexes of weathering CIW = 58–93 (Harnois, 1988) and CIA = 48–80 (Nesbitt and Young, 1982; Visser and Young, 1990) (Table 2) indicate that rocks in the source areas were likely transformed to varying degrees by processes of chemical weathering.

There are specific regularities in the distribution of rare earth elements (REEs) in the studied rocks. For

Table 2. Minimum and maximum values of some geochemical parameters and petrochemical modules and indexes calculated for Upper Proterozoic and Lower Paleozoic terrigenous deposits of the Lesser Khingan terrane

Parameters		Iginchi Formation	Murandavi Formation	Kimkan sequence
ΣREE	min	98	132	128
	max	194	222	240
$[La/Yb]_n$	min	15.13	6.45	5.61
	max	39.92	41.62	11.79
$[Gd/Yb)_n$	min	3.02	1.59	1.54
	max	8.04	9.47	2.67
Eu/Eu*	min	0.55	0.53	0.33
	max	0.76	0.83	0.47
AM	min	0.12	0.14	0.17
	max	0.24	0.21	0.24
HM	min	0.23	0.24	0.22
	max	0.36	0.36	0.36
FM	min	0.10	0.10	0.06
	max	0.14	0.17	0.16
TM	min	0.06	0.06	0.03
	max	0.08	0.08	0.05
SPM	min	0.25	0.24	0.34
	max	0.43	0.57	0.48
CIW	min	59.39	59.18	58.06
	max	85.35	77.68	65.73
CIA	min	52.59	47.69	52.04
	max	71.63	68.37	55.29

AM = Al_2O_3/SiO_2 (Ketris, 1976), HM = $(Al_2O_3 + TiO_2 + Fe_2O_3 + FeO + MnO)/SiO_2$ (Yudovich et al., 1977), FM = $(Fe_2O_3 + FeO + MgO)/SiO_2$ (Yudovich, 1981), TM = TiO_2/Al_2O_3 (Migdisov, 1960), SPM = $(Na_2O + K_2O)/Al_2O_3$ (Yudovich, 1981), CIW = $100 \times Al_2O_3/(Al_2O_3 + CaO + Na_2O)$ (Hanois, 1988), CIA = $(Al_2O_3/(Al_2O_3 + CaO + Na_2O + K_2O)) \times 100$ (Nessbit and Young, 1982; Visser and Young, 1990).

example, sandstones and silty sandstones of the Iginchi Formation are depleted in rare earth elements (ΣREE = 98–194 ppm) compared with the overlying sediments of the Murandavi Formation (ΣREE = 132–222 ppm) and the Kimkan sequence (ΣREE = 128–240 ppm) (Table 2), which is, first of all, due to a relative depletion in the first heavy REEs (Fig. 4). In accordance with this, the La/Yb ratio decreases up the section from 15–40 (Iginchi Formation) to 5.6–11.8 (Kimkan sequence). In the same direction, the Eu/Eu* ratio increases (Fig. 4) from 0.55–0.76 (Iginchi Formation) to 0.33–0.47 (Kimkan sequence) (Table 2).

The distribution plots of concentrations of trace elements normalized to the upper continental crust composition in silty sandstones and sandstones of the Iginchi Formation and sandstones of the Murandavi Formation are similar, except for the higher concentrations of heavy rare earths in the latter. Furthermore, these rocks contain Rb, Ba, U, Th, Zr, LREE, and Pb in concentrations similar to those in the upper continental crust at distinct relative depletion in Sr, Nb, Ta, and Yb (Figs. 5a and 5b). As seen in the spider diagram (Fig. 5c), silty sandstones and sandstones of the Kimkan sequence are characterized by higher concentrations of most of the lithophile elements, except for the negative anomalies of Nb, Ta, and Sr. This geochemical feature allows us to assume that these rocks are

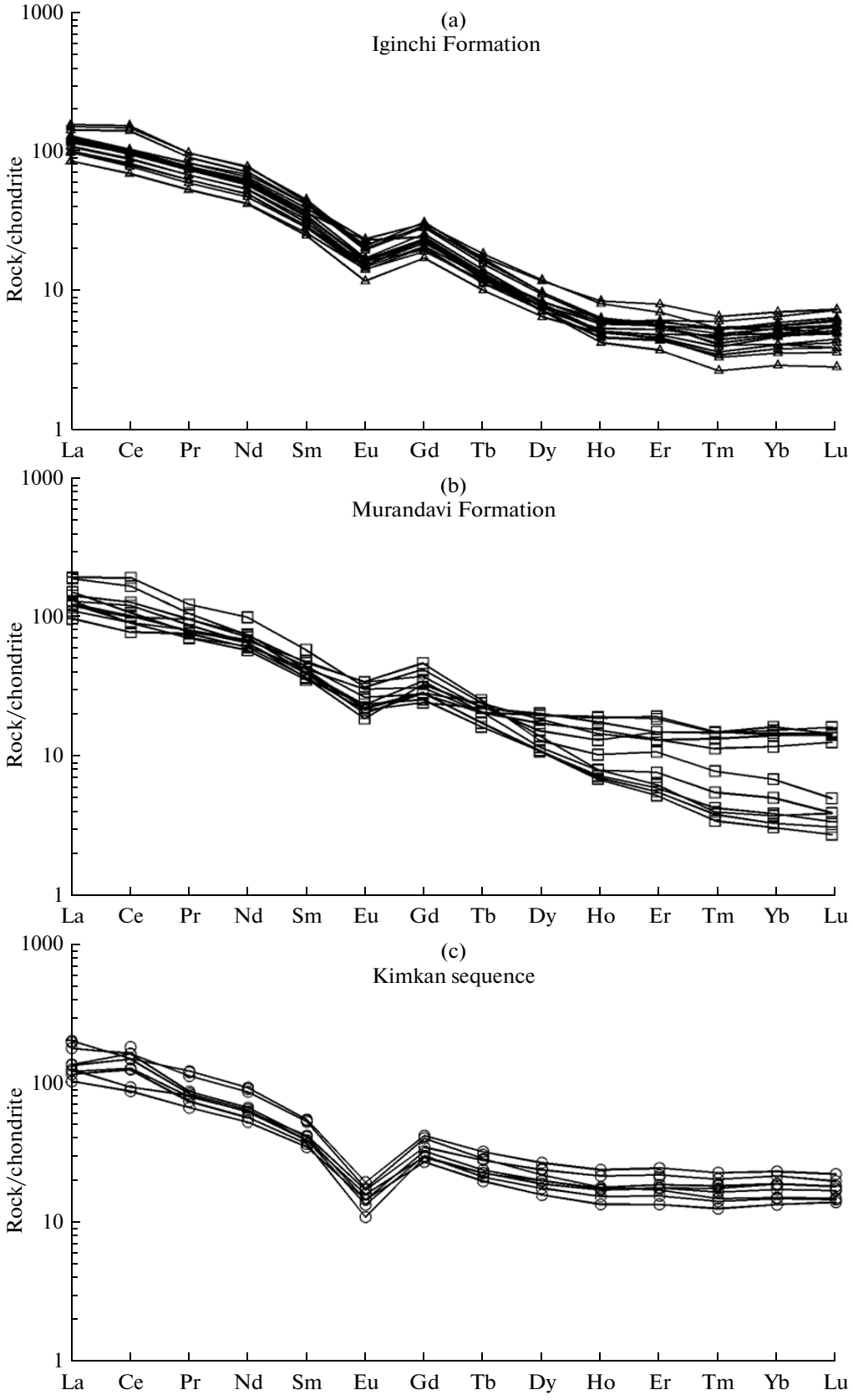

Fig. 4. Chondrite-normalized REE distribution plot in terrigenous rocks of the Khingan Group of the Lesser Khingan Terrane (McDonough and Sun, 1995).

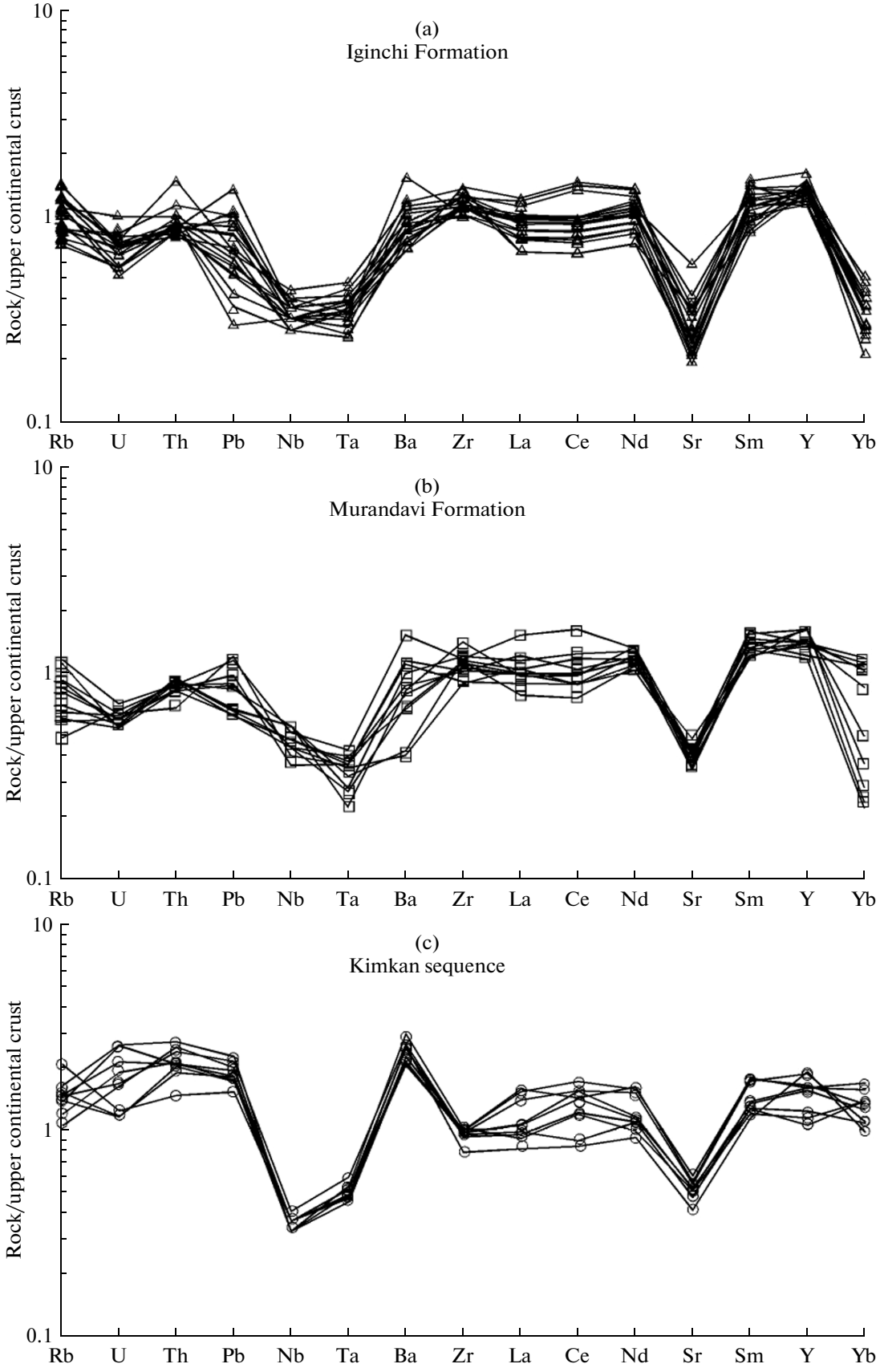

Fig. 5. Spider diagrams compiled for terrigenous rocks of the Khingan Group of the Lesser Khingan Terrane. The composition of the upper continental crust is given after (Taylor and McLennan, 1985).

close to the deposits of the underlying Iginchi and Murandavi formations (Figs. 5a and 5b).

PALEORECONSTRUCTION OF SOURCE AREAS AND GEODYNAMIC SETTINGS OF SEDIMENTATION

In order to identify the compositions of rocks in source areas, the diagrams of distribution of macrocomponents and trace elements are usually used. In particular, the positions of figurative points of compositions of terrigenous rocks of the Khingan Group on the diagrams of (Na_2O–CaO–K_2O) and (CaO + MgO)–SiO_2/10–(Na_2O + K_2O) (Figs. 6a and 6b), based on the silica–alkalis ratio in sediments, indicate that a source area during the period of sedimentation was composed of felsic rocks (in particular, granite). Only a few points of sandstones from the Iginchi Formation are close to the field of recycled sediments (Fig. 6a). A similar conclusion can be drawn from the analysis of discrimination diagrams plotted on the basis of the behavior of lithophile elements, such as La, Th, Sc, Ti, Zr, Nb, and Y (Figs. 7c–7d), and a factor diagram (Fig. 6f).

In order to reconstruct paleogeodynamic settings of sedimentation, a series of discrimination diagrams was developed. They include the commonly used diagrams based on the tendencies of decreasing $Fe_2O_3^*$ + MgO, TiO_2, and Al_2O_3/SiO_2 values and increasing K_2O/Na_2O and $Al_2O_3/(CaO + Na_2O)$ values from sandstones of oceanic island arcs to those in the island arcs developed on the continental crust, and then to the active and passive continental margins (*Interpretatsiya...*, 2001; etc.). As seen in these diagrams (Fig. 7), terrigenous rocks of the Khingan Group are characterized by moderate values of $Fe_2O_3^*$ + MgO, Al_2O_3/SiO_2, K_2O/Na_2O, and $Al_2O_3/(CaO + Na_2O)$ and they are attributed to sediments which formed in the island arc settings developed on the continental crust and at the active continental margin. An analysis of ternary and binary discriminatory diagrams (Fig. 8) based on the distribution of trace elements leads to similar conclusions.

RESULTS OF U-Pb GEOCHRONOLOGY

In total, 105 grains of detrital zircons were extracted from polymictic silty sandstone of the Iginchi Formation (Sample C-1167), 92 grains of which yielded concordant age values. As seen in Figs. 9 and 10, Late Riphean (960–767 Ma) zircons (73%) dominate, whereas Middle and Early Riphean zircons (1.59–1.12 Ga, 13%) and Early Proterozoic zircons (2.18–1.69 Ga, 14%) are in subordinate amounts and they do not form distinct peaks on the age histogram (Fig. 9).

We extracted 115 detrital zircons from polymictic sandstones of the Murandavi Formation, 94 of which yielded concordant age values. Most of these zircons (74%) have Late Riphean age (954–652 Ma) (Figs. 9 and 11). There are only a few grains (2%) of Middle and Late Riphean zircons (1.55–1.09 Ga). In spite of a large proportion (24%) of Early Proterozoic zircons (2.50–1.70 Ga), they do not form distinct age peaks on the age histogram (Fig. 9).

Only 52 grains from 105 detrital zircons extracted from polymictic silty sandstone of the Kimkan sequence (Sample C-1165) yielded concordant age values, among which the unified population of Early Paleozoic and Vendian zircons is clearly dominant (66%; 638–481 Ma) (Figs. 9 and 12). As seen in the histogram (Fig. 9), a group of Late Riphean zircons (957–881 Ma, 23%) dominates, while more ancient zircons (1.66–1.06 Ga) are present in a smaller amount (11%).

DISCUSSION OF RESULTS

The material composition of sedimentary complexes is one of the least studied aspects in the history of the formation of the Central Asian Fold Belt. The modern structural plan shows that these complexes are fragments of the ancient vast basins, and their geochemical characteristics are a quite sensitive indicator of geodynamic conditions of sedimentation. According to current ideas, the thick terrigenous sequences are the most applicable sites for the reconstruction of geodynamic conditions of their formation. The study of such objects allows one to identify the main features of the evolution of sedimentary basins and thus trace the evolution of geodynamic conditions for a long period of sedimentation. However, the experience of studying sedimentary complexes of the Central Asian Fold Belt shows that the study of sedimentary complexes even small in thickness and the period of sedimentation makes it possible to clarify the tectonic evolution of the major geological structures (He et al., 2005; Meng et al., 2010; Zhou et al., 2010; Han et al., 2011; Sorokin et al., 2012, 2015; Maslov et al., 2012, 2013, 2015; Kozakov et al., 2013; Chumakov et al., 2013; Zhou and Wilde, 2013; Smirnova et al., 2013; Smirnova and Sorokin (in press); etc.).

The paleoreconstruction of geological processes that occurred in the Late Precambrian and Early Paleozoic is of particular importance, since orogenic complexes in Central Asia began to form from the Late Precambrian (Mossakovskii et al., 1993; Didenko et al., 1994; Parfenov et al., 2003; etc.).

The "key objects" in the structure of the Lesser Khingan Terrane which can significantly clarify the Late Precambrian history of the Central Asian Fold Belt include the Upper Riphean–Cambrian Khingan Group. The results of study of the latter are discussed in this article.

As follows from the results obtained, the youngest detrital zircons from the terrigenous deposits of the Iginchi and Murandavi formations yield the Late

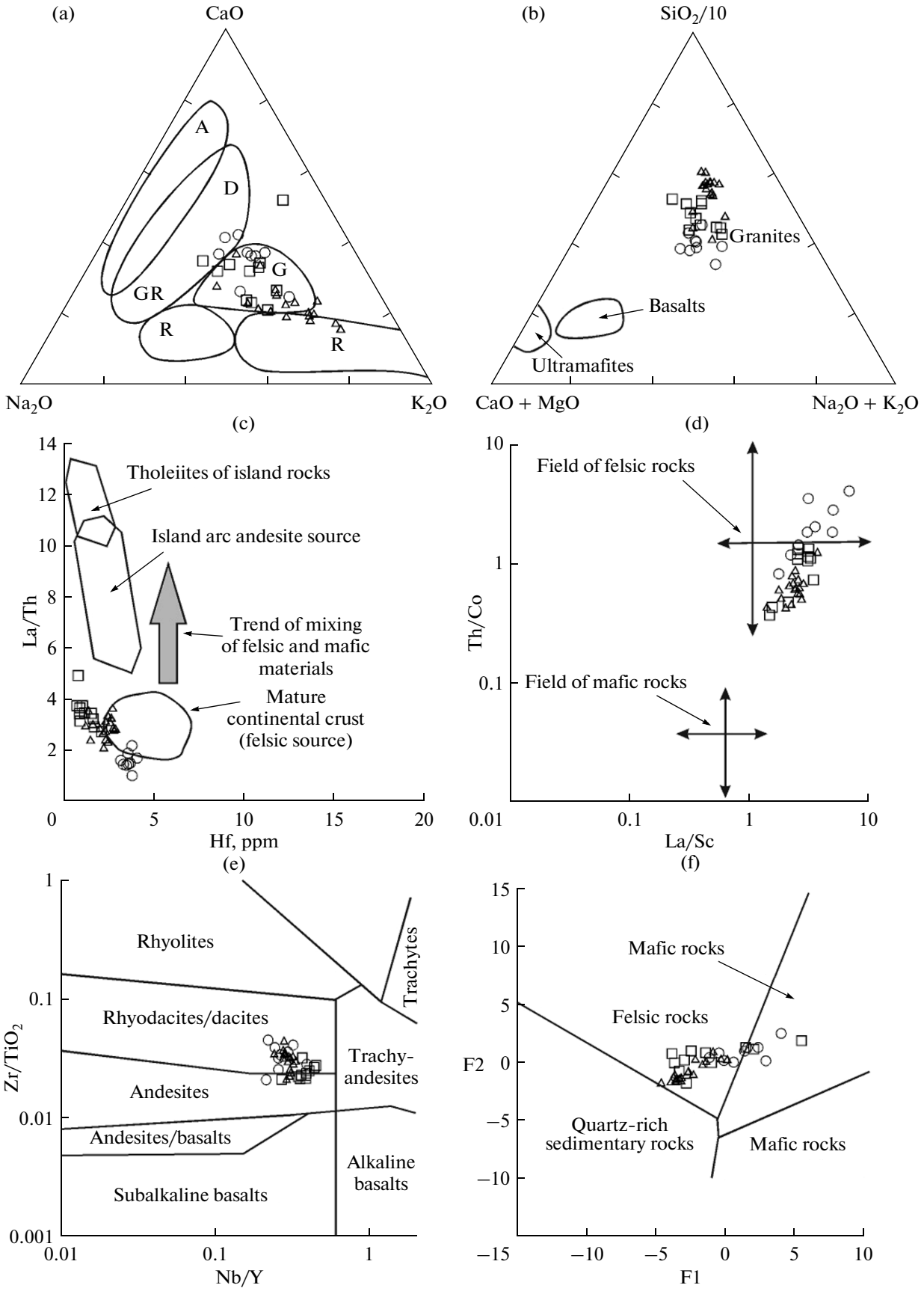
(a)
CaO
A
D
G
GR
R
R
Na2O
K2O
(b)
SiO2/10
Granites
Basalts
Ultramafites
CaO + MgO
Na2O + K2O
(c)
Tholeiites of island rocks
Island arc andesite source
Trend of mixing of felsic and mafic materials
Mature continental crust (felsic source)
La/Th
Hf, ppm
(d)
Field of felsic rocks
Field of mafic rocks
Th/Co
La/Sc
(e)
Rhyolites
Trachytes
Rhyodacites/dacites
Trachy-andesites
Andesites
Andesites/basalts
Alkaline basalts
Subalkaline basalts
Zr/TiO2
Nb/Y
(f)
Mafic rocks
Felsic rocks
Quartz-rich sedimentary rocks
Mafic rocks
F2
F1

Fig. 6. Set of diagrams compiled for terrigenous rocks of the Khingan Group of the Lesser Khingan Terrane: (a) Na_2O–CaO–K_2O (Bhatia, 1983), (b) (CaO + MgO)–$SiO_2/10$–(Na_2O + K_2O) (Taylor and McLennan, 1985), (c) Hf–La/Th (Gu, 1994; Nath et al., 2000), (d) La/Sc–Th/Co (Cullers, 2002), (e) Nb/Y–Zr/TiO_2 (Winchester and Floyd, 1977), (f) F1–F2 (Roser and Korsch, 1988). Fig. 6a: the following fields are shown: A—andesites, D—dacites, GR—granodiorites, G—granites, R—reduced sediments. Fig. 6f: $F1 = 30.638 \times (TiO_2/Al_2O_3) - 12.541 \times (Fe_2O_3total/Al_2O_3) + 7.329 \times (MgO/Al_2O_3) + 12.031 \times (Na_2O/Al_2O_3) + 35.402 \times (K_2O/Al_2O_3) - 6.382$; $F2 = 56.5 \times (TiO_2/Al_2O_3) - 10.879 \times (Fe_2O_3total/Al_2O_3) + 30.875 \times (MgO/Al_2O_3) - 5.404 \times (Na_2O/Al_2O_3) + 11.112 \times (K_2O/Al_2O_3) - 3.8$.

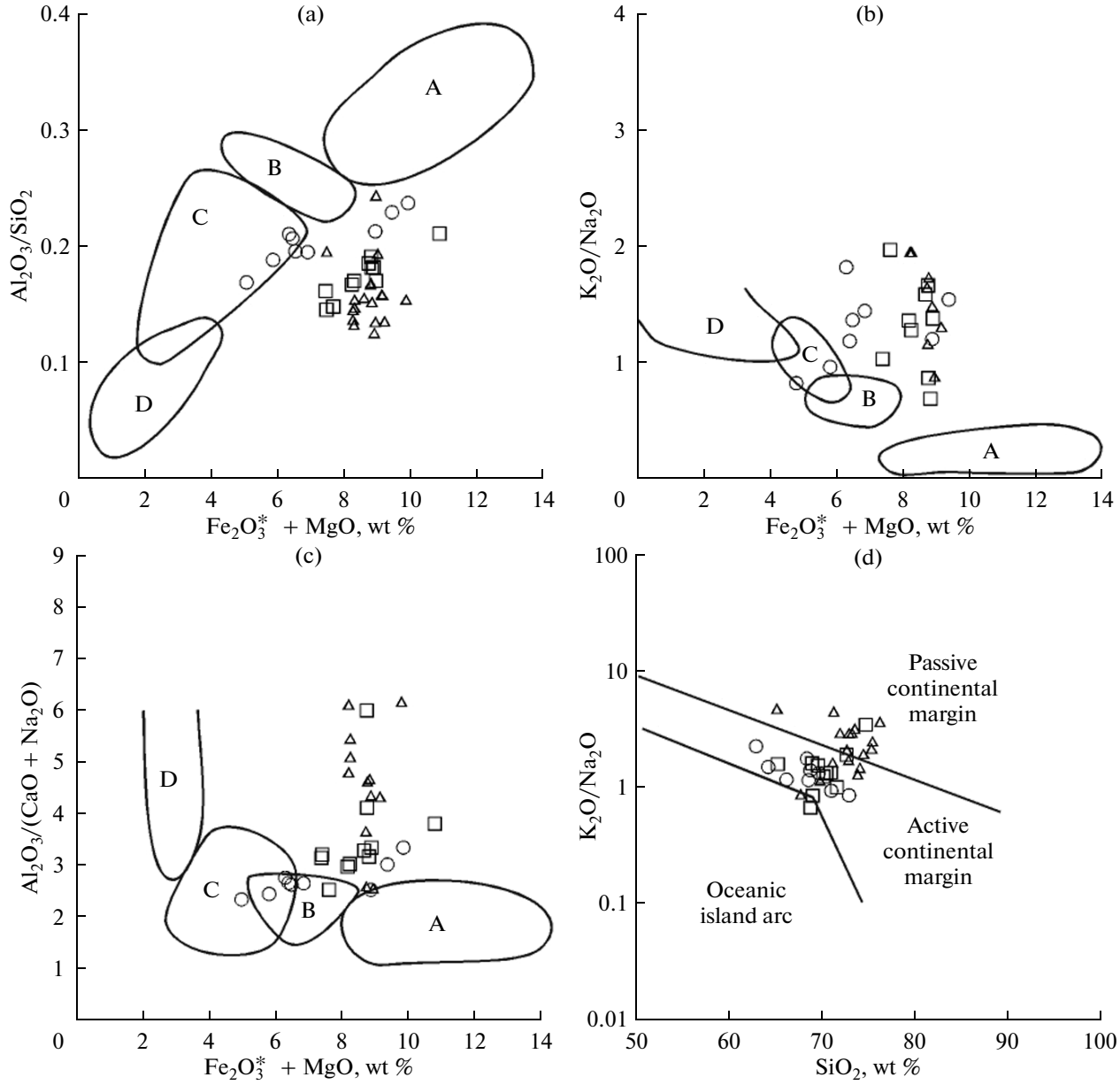

Fig. 7. Diagrams plotted for terrigenous rocks of the Khingan Group of the Lesser Khingan Terrane: (a) ($Fe_2O_3^*$ + MgO)–Al_2O_3/SiO_2, (b) ($Fe_2O_3^*$ + MgO)–K_2O/Na_2O, (c) ($Fe_2O_3^*$ + MgO)–$Al_2O_3/(CaO + Na_2O)$ (Bhatia, 1983), (d) SiO_2–K_2O/Na_2O (Roser and Korsch, 1986). See legend in Fig 3. $Fe_2O_3^*$—total iron. Fields of sandstones from the fiollowing tectonic settings: A—oceanic island arcs, B—continental island arcs, C—active continental margins, D—passive continental margins.

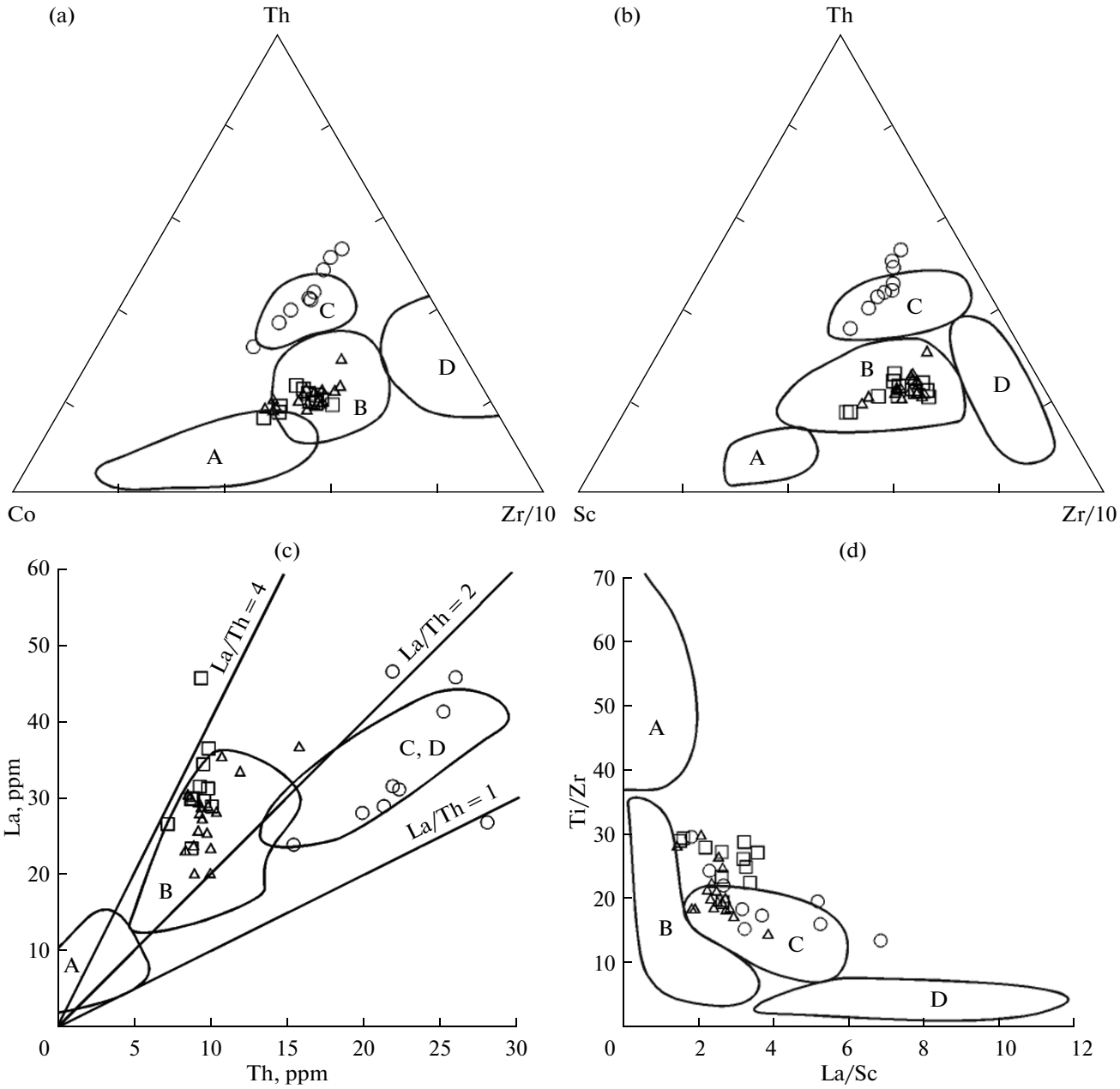

Fig. 8. Diagrams compiled for terrigenous rocks of the Khingan Group of the Lesser Khingan Terrane: (a) Co–Th–Zr, (b) Sc–Th–Zr/10, (c) Th–La, (d) La/Sc–Th/Zr (Bhatia and Crook, 1986). See legend in Fig. 3. Fields of sandstones from the following tectonic settings: A—oceanic island arcs, B—continental island arcs, C—active continental margins, D—passive continental margins.

Riphean age. It should be recalled that the deposits of the Murandavi Formation are intruded by granite bodies with age of 535 ± 6 Ma (Sorokin et al. (in press)). According to this, the upper age boundary of the Murandavi and underlying Iginchi formations is the Vendian–Cambrian boundary. Thus, it should be accepted that the age of these formations is the Late Riphean–Vendian.

The Late Riphean zircon population is present in the deposits of the Kimkan sequence. However, these deposits contain younger zircons of Vendian–Early

Fig. 9. Histograms and curves of relative probability of ages of detrital zircons from silty sandstone of the Kimkan sequence (Sample S-1165), sandstone of the Murandavi Formation (Sample Yu-72-5), and silty sandstone of the Iginchi Formation (Sample S-1167) of the Khingan Group of the Lesser Khingan Terrane.

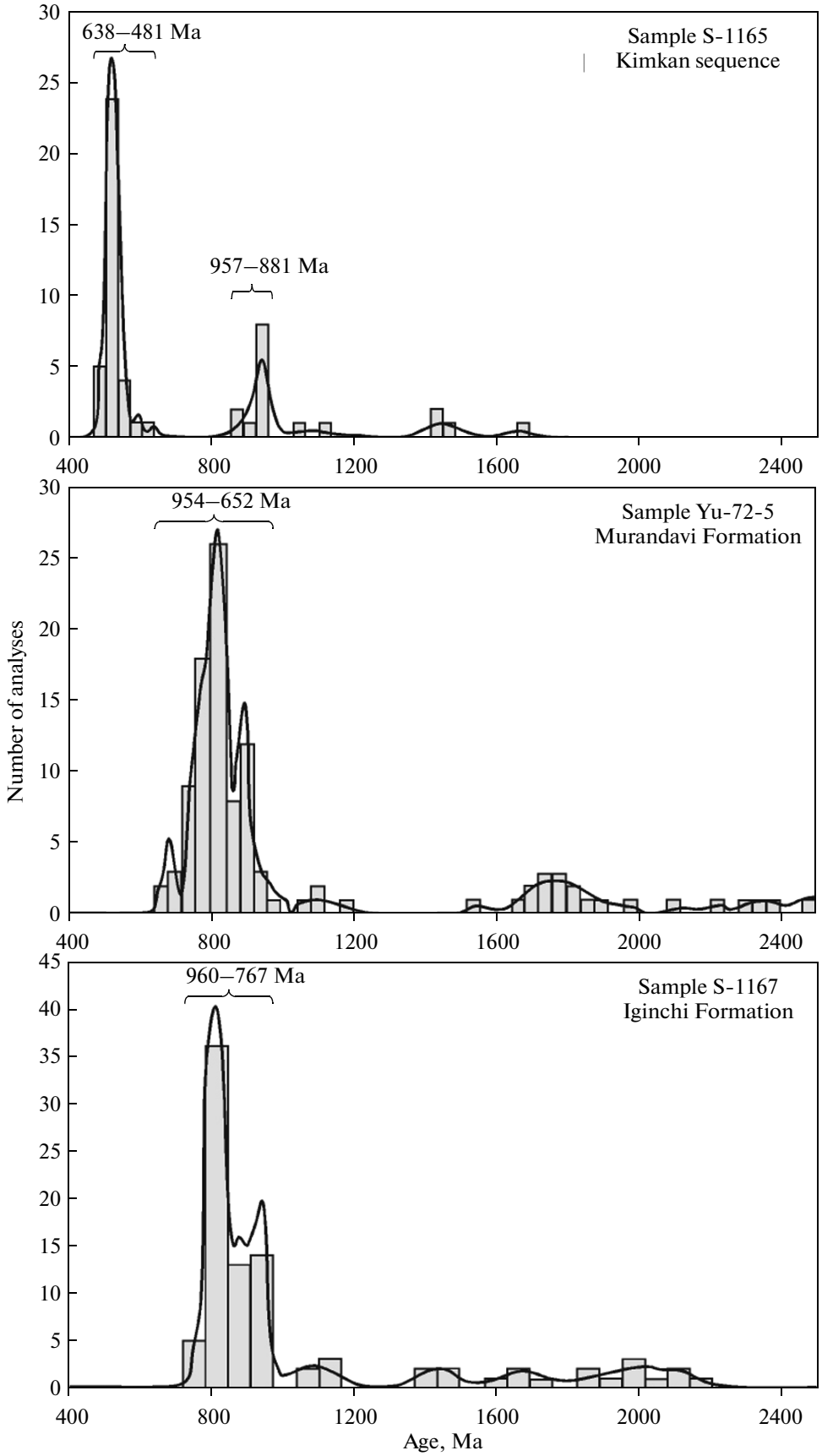
638–481 Ma
957–881 Ma
Sample S-1165
Kimkan sequence
954–652 Ma
Sample Yu-72-5
Murandavi Formation
960–767 Ma
Sample S-1167
Iginchi Formation
Number of analyses
Age, Ma

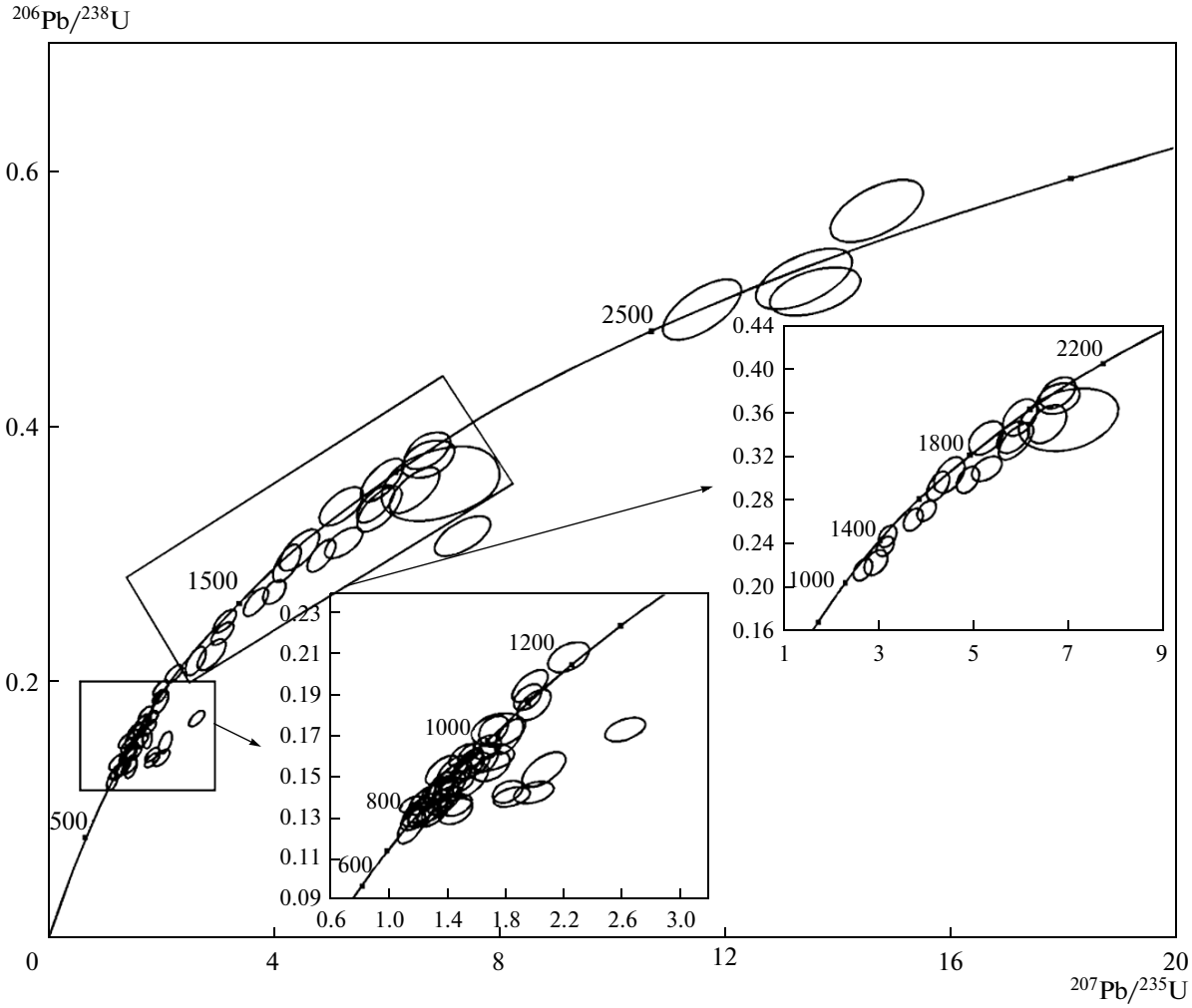

Fig. 10. Concordia diagram for detrital zircons from silty sandstone of the Iginchi Formation (Sample S-1167) of the Khingan Group of the Lesser Khingan Terrane.

Ordovician age. This indicates that deposits of this sequence have younger age than those of Murandavi and Iginchi formations. Given the fact that the deposits of the Khingan Group, as a whole, and the Kimkan sequence, in particular, are intruded by Early Paleozoic intrusions with ages varying in the range of 480–429 Ma (see above), one can suggest with confidence that the accumulation of deposits of the Kimkan sequence occurred in the Late Cambrian–Early Ordovician.

Thus, the geochronological data obtained make it possibly to clarify the age boundaries of stratigraphic units which are attributed to the Khingan Group of the Lesser Khingan Terrane of the eastern part of the Central Asian Fold Belt. Thus, it is clear that the Murandavi and underlying Iginchi formations belong to the Late Riphean–Vendian and the Kimkan sequence belongs to the Late Cambrian–Early Ordovician.

The periods of formation of the Murandavi and Iginchi formations, on one hand, and the Kimkan sequence, on the other hand, are separated by the stage of granitoid magmatism at the turn of the Vendian–Cambrian. Because of this, they cannot be attributed to a unified sedimentary sequence.

Mineralogical and geochemical characteristics (Fig. 6) of terrigenous rocks of the Iginchi and Murandavi formations and Kimkan sequence show that, in the source areas during the period of sedimentation, felsic rocks dominated. On the basis of the fact that the studied deposits are characterized by model ages of $t_{Nd(DM)} = 1.5–1.7$ Ga at negative $\varepsilon_{Nd(0)} = -9.3$ to -11.4 (Table 3), one can assume that the main sources of these deposits were Early Riphean complexes and (or) the younger igneous rocks, the primary melts of which resulted from the reworking of the continental crust of a particular age.

The analysis of discrimination diagrams shows that the sedimentation of deposits of the Iginchi and Murandavi formations and Kimkan sequence occurred most likely in a subduction setting, namely, the island

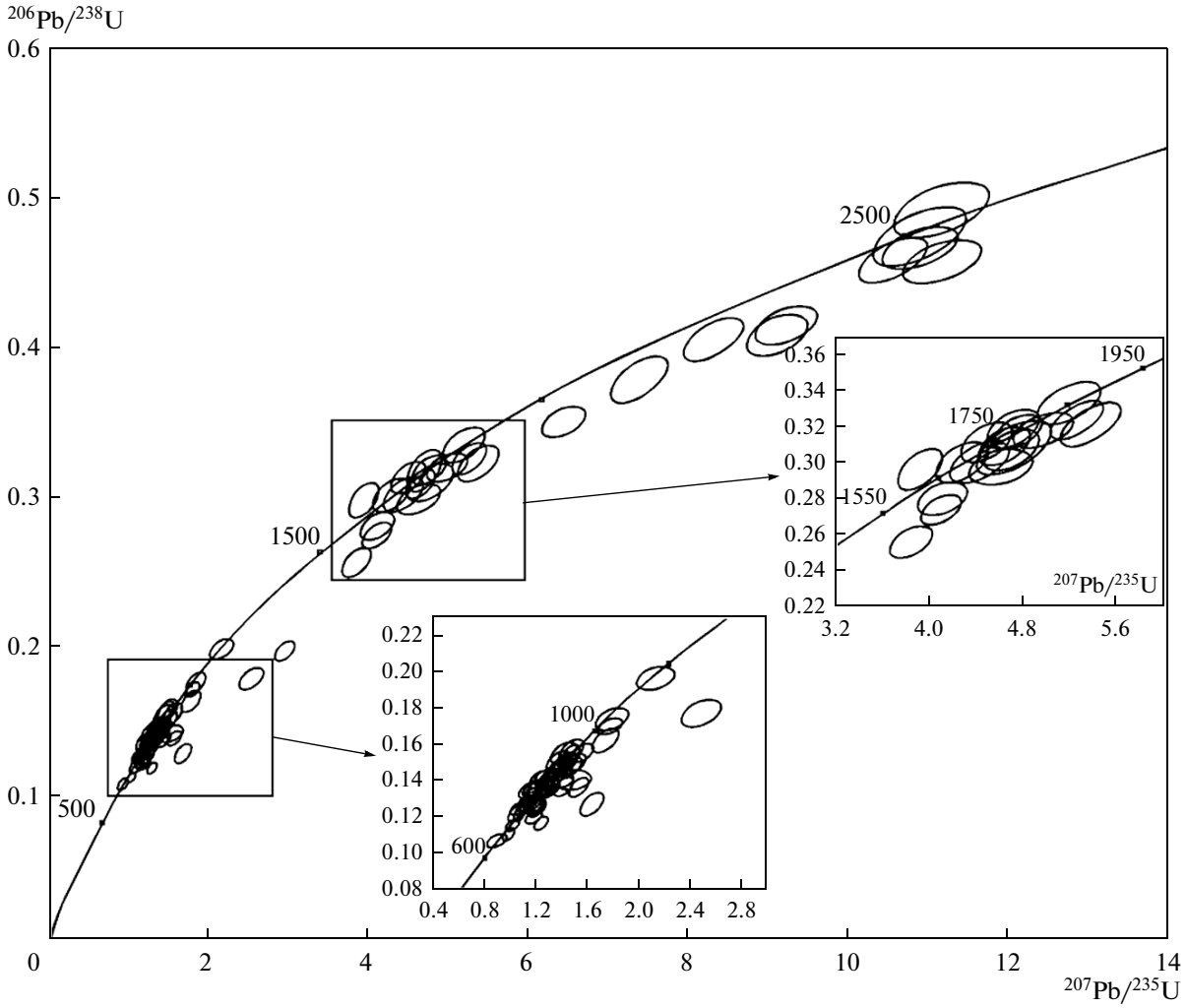

Fig. 11. Concordia diagram for detrital zircons from sandstone of the Murandavi Formation (Sample Yu-72-5) of the Khingan Group of the Lesser Khingan Terrane.

arc developed on the continental crust and (or) at the active continental margin (Figs. 7 and 8), which is consistent with the composition of greywacke sediments. Moreover, this interpretation is confirmed by the fact that sedimentation occurred against the backdrop of magmatic activity, as evidenced by the presence of Late Riphean zircons in sandstones and silty sandstones of the Iginchi and Murandavi formations and Vendian–

Table 3. Sm-Nd isotope geochronology of Upper Proterozoic and Lower Paleozoic terrigenous deposits of the Lesser Khingan terrane

Sample	Rock	Formation	Sm	Nd	$^{147}Sm/^{144}Nd$	$^{143}Nd/^{144}Nd$	$\varepsilon_{Nd(0)}$	$t_{Nd(DM)}$
S-1165	Silty sandstone	Kimkan sequence	7.89	40.75	0.1171	0.512054 ± 3	–11.4	1725
S-1165-1	Silty sandstone	Kimkan sequence	8.09	42.07	0.1163	0.512088 ± 3	–10.7	1659
S-1170	Sandstone	Murandavi Formation	8.46	44.5	0.1150	0.512161 ± 2	–9.3	1527
S-1167	Silty sandstone	Iginchi Formation	6.13	31.52	0.1177	0.512118 ± 1	–10.1	1636
S-1167-1	Sandstone	Iginchi Formation	5.12	27.02	0.1146	0.512121 ± 2	–10.1	1581
S-1168	Silty sandstone	Iginchi Formation	6.11	31.65	0.1166	0.512101 ± 2	–10.5	1645
S-1169	Sandstone	Iginchi Formation	6.26	34.18	0.1107	0.512098 ± 3	–10.5	1555

Errors (2σ) in determining $^{143}Nd/^{144}Nd$ correspond to the last significant digits after the decimal point.

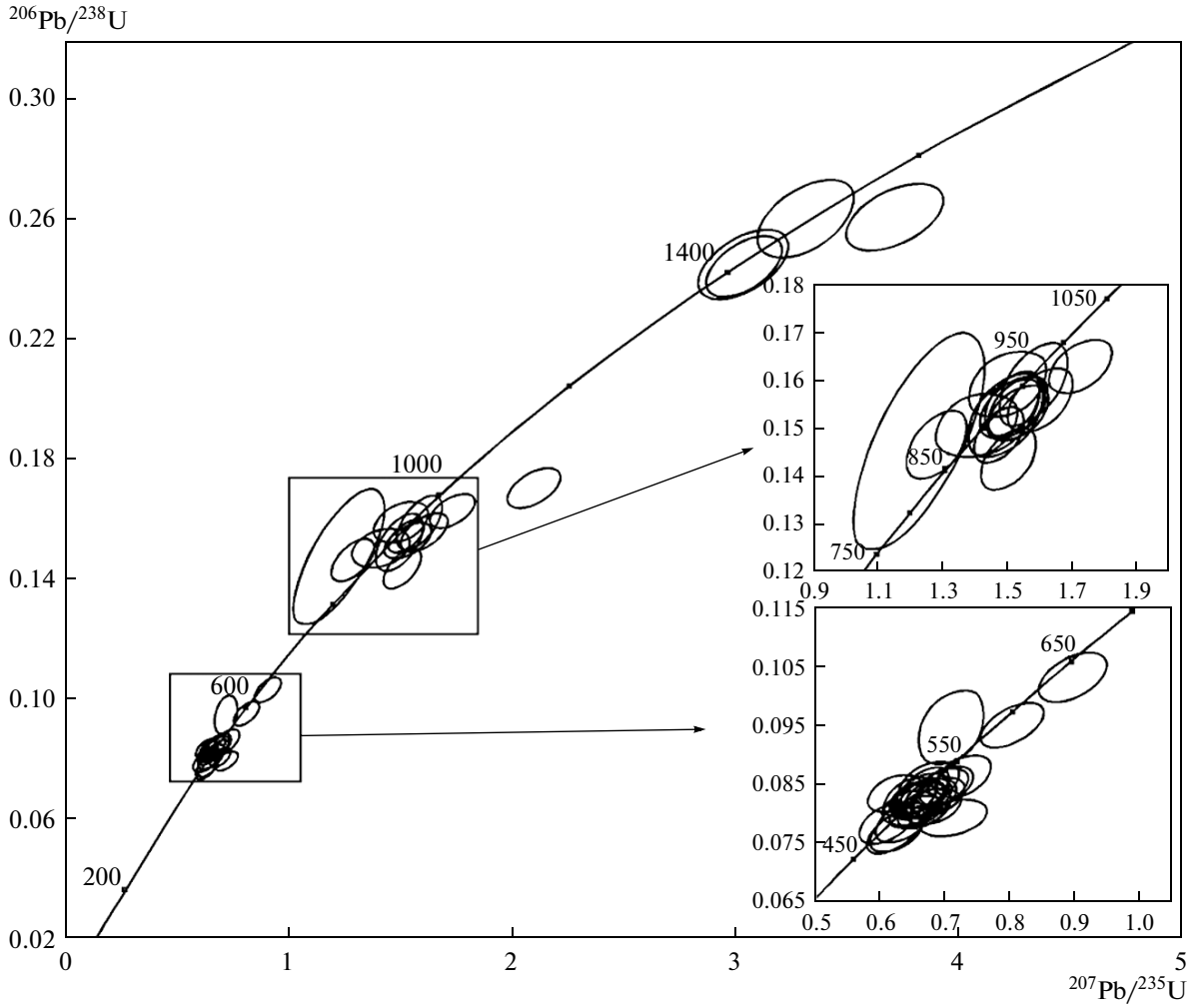

Fig. 12. Concordia diagram for detrital zircons from silty sandstone from the Kimkan sequence (Sample S-1165) of the Khingan Group of the Lesser Khingan Terrane.

Early Ordovician zircons in deposits of the Kimkan sequence.

CONCLUSIONS

On the basis of the results of our research, the following conclusions were made:

(1) The ages of the Murandavi and underlying Iginchi formations are Late Riphean–Vendian; the age of the Kimkan sequence is Late Cambrian–Early Ordovician.

(2) The deposits of Iginchi and Murandavi formations, on one hand, and the Kimkan sequence, on the other hand, vary greatly in age, and the periods of formation of these complexes are separated by the stage of granitoid magmatism at the turn of the Vendian–Cambrian. Because of this, they cannot be attributed to a unified sedimentary sequence.

(3) It is the most probable that the sedimentation of the Iginchi and Murandavi formations and the Kimkan sequence occurred under subduction conditions against the backdrop of magmatic activity.

ACKNOWLEDGMENTS

We are grateful to the staff of the analytical laboratories of the Institute of Geology and Nature Management (V.I. Rozhdestvina, E.N. Voropaeva, O.G. Medvedeva, A.I. Palazhchenko, E.S. Sapozhnik, E.V. Ushakova), Institute of Tectonics and Geophysics (L.S. Bokovenko, E.M. Golubeva, A.V. Shtareva), and Institute of Precambrian Geology and Geochronology (N.Yu. Zagornaya and L.B. Terentieva) for assistance in the analytical research.

This work was supported by Russian Foundation for Basic Research (project no. 14-05-00209).

Reviewers I.M. Gorokhov and M.G. Leonov

REFERENCES

Bhatia, M.R., Plate tectonics and geochemical composition of sandstones, *J. Geol.*, 1983, vol. 91, no. 6, pp. 611–627.

Bhatia, M.R. and Crook, K.A.W., Trace element characteristics of graywackes and tectonic setting discrimination of sedimentary basins, *Contrib. Mineral. Petrol.*, 1986, vol. 92, pp. 181–193.

Bi, J.H., Ge, W.C., Yang, H., et al., Petrogenesis and tectonic implications of early Paleozoic granitic magmatism in the Jiamusi Massif, NE China: geochronological, geochemical and Hf isotopic evidence, *Asian J. Earth Sci.*, 2014, vol. 96, pp. 308–331.

Black, L.P., Kamo, S.L., Allen, C.M., et al., Improved $^{206}Pb/^{238}U$ microprobe geochronology by the monitoring of trace-element-related matrix effect: SHRIMP, ID-TIMS, ELA-ICP-MS and oxygen isotope documentation for a series of zircon standards, *Chem. Geol.,* 2004, vol. 205, pp. 15–140.

Buchko, I.V., Sorokin, A.A., and Kudryashov, N.M., Late Paleozoic gabbroids of the Malokhingansk Terrane in the eastern area of the Central Asian Fold Belt: first geochronological data, *Dokl. Earth Sci.*, 2011, vol. 440, no. 2, pp. 1298–1302.

Buchko, I.V., Sorokin, A.A., and Kudryashov, N.M., Age and tectonic position of the Early Paleozoic Malyi Khingan Terrane in the eastern part of the Central Asian Fold Belt, *Dokl. Earth Sci.* 2012, vol. 445, no. 2, pp. 929–933.

Buchko, I.V., Sorokin, A.A., and Kudryashov, N.M., Late Paleozoic gabbroids of the Lesser Khingan terrane of the eastern Central-Asian fold belt: Age, geochemistry, and tectonic setting, *Russ. J. Pac. Geol.*, 2013, vol. 7, no. 3, pp. 189–198.

Chumakov, N.M., Pokrovskii, B.G., and Maslov, A.V., Stratigraphic position and significance of carbonate rocks related to Neoproterozoic glacial horizons of the Urals, *Stratigr. Geol. Correl.*, 2013, vol. 21, no. 6, pp. 573–591.

Cullers, R.L., Implications of elemental concentrations for provenance, redox conditions, and metamorphic studies of shales and limestones near Pueblo, CO, USA, *Chem. Geol.*, 2002, vol. 191, pp. 305–327.

Didenko, A.N., Mossakovskii, A.A., Pecherskii, D.M., et al., Geodynamics of the Central Asian oceans in the Paleozoic, *Geol. Geofiz.*, 1994, nos. 7–8, pp. 59–75.

Dobkin, S.N., *Gosudarstvennaya geologicheskaya karta Rossiiskoi Federatsii masshtaba 1: 200000. Izdanie vtoroe. Bureinskaya seriya. N-52-XXX (Obluch'e)* (The 1 : 200000 State Geological Map of the Russian Federation, the 2nd Ed. Bureya Series. Sheet N-52-XXX (Obluch'e)), Vas'kin, A.F., Ed., St. Petersburg: Vseross. Nauchno-Issled. Geol. Inst., 2000 [in Russian].

Gehrels, G., Detrital zircon U-Pb geochronology: current methods and new opportunities, in *Tectonics of Sedimentary Basins: Recent Advances*, Busby, C. and Perez, A.A., Eds., Hoboken, New Jersy: Wiley-Blackwell, 2011, pp. 45–62.

Geodinamika, magmatizm i metallogeniya vostoka Rossii (The Geodynamics, Magmatism and Metallogeny of the East Russia), Khanchuk, A.I., Ed., Vladivostok: Dal'nauka, 2006 [in Russian].

Goldstein, S.J. and Jacobsen, S.B., Nd and Sr isotopic systematics of rivers water suspended material: implications for crustal evolution, *Earth Planet. Sci. Lett.*, 1988, vol. 87, pp. 249–265.

Gu, X.X., Geochemical characteristics of the Triassic Tethys turbidites in northwestern Sichuan, China: implications for provenance and interpretation of the tectonic setting, *Geochim. Cosmochim. Acta*, 1994, vol. 58, pp. 4615–4631.

Han, G., Liu, Y., Neubauer, F., et al., Origin of terranes in the eastern Central Asian Orogenic Belt, NE China: U-Pb ages of detrital zircons from Ordovician–Devonian sandstones, North Da Xing'an Mts., *Tectonophysics*, 2011, vol. 511, pp. 109–124.

Harnois, L., The CIW index: a new chemical index of weathering, *Sediment. Geol.*, 1988, vol. 55, nos. 3–4, pp. 319–322.

He, Z.J., Li, J.Y., Mo, S.G., and Sorokin, A.A., Geochemical discriminations of sandstones from the Mohe foreland basin, northeastern China: tectonic setting and provenance, in *Sci. China, Ser. D: Earth Sci.*, 2005, vol. 48, no. 5, pp. 613–621.

Herron, M.M., Geochemical classification of terrigenous sands and shales from core or log data, *J. Sediment. Petrol.*, 1988, vol. 58, pp. 820–829.

Interpretatsiya geokhimicheskikh dannykh (Interpretation of the Geochemical Data), Sklyarov, E.V., Ed., Moscow: Internet Inzh., 2001, vol. 1 [in Russian].

Jacobsen, S.B. and Wasserburg, G.J., Sm-Nd evolution of chondrites and achondrites. II, *Earth Planet. Sci. Lett.*, 1984, vol. 67, pp. 137–150.

Ketris, M.P., Petrochemical properties of terrigenous rocks, in *Tr. Inst. geol. Komi filiala AN SSSR "Ezhegodnik-1974"* (Proc. Inst. Geol. Komi Branch Akad. Nauk USSR "Yearbook-1974"), Moscow: Vsesoyuz. Inst. Nauchno–Techn. Inform. Akad. Nauk USSR, 1976, pp. 32–38.

Kossovskaya, A.G. and Tuchkova, M.I., The problem of mineralogical–petrochemical classification and genesis of sandy rocks, *Litol. Polezn. Iskop.*, 1988, no. 2, pp. 8–24.

Kotov, A.B., Velikoslavinskii, S.D., Sorokin, A.A., et al., Age of the Amur group of the Bureya-Jiamusi Superterrane in the Central Asian Fold Belt: Sm-Nd isotope evidence, *Dokl. Earth Sci.*, 2009a, vol. 429, no. 8, pp. 1245–1248.

Kotov, A.B., Sorokin, A.A., Salnikova, E.B., et al., Early Paleozoic age of gabbroids of the Amur complex (Bureya-Jiamusi Superterrane of the Central Asian Fold Belt), *Dokl. Earth Sci.*, 2009b, vol. 425, no. 1, pp. 185–188.

Kozakov, I.K., Salnikova, E.B., Kovach, V.P., et al., Late Riphean age of conglomerates from the Kholbonur complex of Songino block, Central Asian Caledonides, *Stratigr. Geol. Correl.*, 2013, vol. 21, no. 5, pp. 482–495.

Ludwig, K.R., Isoplot/Ex, version 2.06. A geochronological toolkit for Microsoft Excel, *Berkley Geochronol. Center Spec. Publ.*, 1999, no. 1a.

Martynyuk, M.V., Ryamov, S.A., and Kondratieva, V.A., *Ob''yasnitel'naya zapiska k skheme korrelyatsii magmaticheskikh kompleksov Khabarovskogo kraya i Amurskoi oblasti* (Explanatory Note to the Correlation Scheme of Magmatic Complexes of the Khabarovsk Krai and the Amur Region), Khabarovsk: Dal'geologiya, 1990 [in Russian].

Maslov, A.V., Vovna, G.M., Kiselev, V.I., et al., U-Pb systematics of detrital zircons from the Serebryanka Group of the Central Urals, *Lithol. Miner. Resour.*, 2012, vol. 47, no. 2, pp. 160–176.

Maslov, A.V., Mizens, G.A., Podkovyrov, V.N., et al., Synorogenic pasammites: major lithochemical features, *Lithol. Miner. Resour.*, 2013, vol. 48, no. 1, pp. 74–97.

Maslov, A.V., Mizens, G.A., Podkovyrov, V.N., et al., Synorogenic clay rocks: Specifics of bulk composition and paleotectonics, *Geochem. Int.*, 2015, vol. 53, no. 6, pp. 510–533.

McDonough, W.F. and Sun, S. S., The composition of the Earth, *Chem. Geol.*, 1995, vol. 120, nos. 3–4, pp. 223–253.

Meng, E., Xu, W.L., Pei, F.P., et al., Detrital-zircon geochronology of Late Paleozoic sedimentary rocks in eastern Heilongjiang Province, NE China: implications for the tectonic evolution of the eastern segment of the Central Asian Orogenic Belt, *Tectonophysics*, 2010, vol. 485, pp. 42–51.

Migdisov, A.A., On the titanium-aluminum ratio in sedimentary rocks, *Geokhimiya*, 1960, no. 2, pp. 149–163.

Mossakovskii, A.A., Ruzhentsev, S.V., Samygin, S.G., and Kheraskova, T.N., Central Asian Fold Belt: geodynamic evolution and formation history, *Geotectonics*, 1994, vol. 27, no. 6, pp. 445–474.

Nath, B.N., Kunzendorf, H., and Pluger, W.L., Influence of provenance, weathering and sedimentary processes on the elemental ratios of the fine-grained fraction of the bedload sediments from the Vembanad Lake and the adjoining continental shelf, southwest coast of India, *J. Sediment. Res.*, 2000, vol. 70, no. 5, pp. 1081–1094.

Nesbitt, H.W. and Young, G.M., Early Proterozoic climates and plate motions inferred from major element chemistry of lutites, *Nature*, 1982, vol. 299, pp. 715–717.

Paces, J.B. and Miller, J.D., Precise U-Pb ages of Duluth Complex and related mafic intrusions, northeastern Minnesota: geochronological insights to physical, petrogenic, paleomagnetic, and tectonomagmatic processes associated with the 1.1 Ga Midcontinent Rift System, *J. Geophys. Res.*, 1993, vol. 98, no. B8, pp. 13997–14013.

Parfenov, L.M., Berzin, N.A., Khanchuk, A.I., et al., Model of formation of orogenic belts in Central and Northeast Asia, *Tikhookean. Geol.*, 2003, vol. 22, no. 6, pp. 7–41.

Pettijohn, F.J., Potter, P.E., Slever, R., *Sand and Sandstone*, Berlin, 1972.

Predovskii, A.A., *Rekonstruktsiya uslovii sedimentogeneza i vulkanizma rannego dokembriya* (Reconstruction of the Conditions of Sedimentation and Volcanism in the Early Precambrian), Leningrad: Nauka, 1980 [in Russian].

Renne, P.R., Swisher, C.C., Deino, A.L., et al., Intercalibration of standards, absolute ages and uncertainties in $^{40}Ar/^{39}Ar$ dating, *Chem. Geol.*, 1998, vol. 45, pp. 117–152.

Resheniya IV Mezhvedomstvennogo regional'nogo stratigraficheskogo soveshchaniya po dokembriyu i fanerozoyu yuga Dal'nego Vostoka i vostochnogo Zabaikal'ya. Komplekt skhem (Resolutions of the IV Interdepartmental Regional Stratigraphical Conference on the Precambrian and Phanerozoic of the Southern Part of the Russian Far East and Eastern Transbaikalia. A Set of Schemes), Khabarovsk: Dal'geologiya, 1994 [in Russian].

Roser, B.P. and Korsch, R.J., Determination of tectonic setting of sandstone-mudstone suites using SiO_2 content and K_2O/Na_2O ratio, *J. Geol.*, 1986, vol. 94, no. 5, pp. 635–650.

Roser, B.D. and Korsch, R.J., Provenance signatures of sandstone-mudstone suites determined using discriminant function analysis of major-element data, *Chem. Geol.*, 1988, vol. 67, pp. 119–139.

Salnikova, E.B., Kotov, A.B., Kovach, V.P., et al., Mesozoic age of the Uril formation of the Amur Group, Lesser Khingan terrane of the Central Asian Foldbelt: results of U-Pb and Lu-Hf isotopic studies of detrital zircons, *Dokl. Earth Sci.*, 2013, vol. 453, no. 2, pp. 1181–1184.

Selivanov, V.A., Svyatogorova, N.N., Baskakova, L.A., et al., *Gosudarstvennaya geologicheskaya karta Rossiiskoi Federatsii. Masshtab 1 : 1000000. M-52(53) Blagoveshchensk* (The 1 : 1000000 State Geological Map of the Russian Federation. Sheet M-52 (53) (Blagoveshchensk)), Zablotskii, E.M., Ed., St. Petersburg: Vseross. Nauchno-Issled. Geol. Inst., 1995 [in Russian].

Smirnova, Yu.N., Sorokin, A.A., Popeko, L.I., and Smirnov, Yu.V., Geochemistry of Paleozoic terrigenous sediments from the Oldoi terrane, eastern Central Asian Orogenic Belt, as an indicator of geodynamic conditions during deposition, *Geochem. Int.*, 2013, vol. 51, no. 4, pp. 306–325.

Smirnova, Yu.N. and Sorokin, A.A., The sources of Upper Proterozoic and Lower Paleozoic terrigenous deposits of the Lesser Khingan Terrane of the Central Asian Fold Belt: results of the LA-ICP-MS U-Pb dating of detrital zircons, *Dokl. Earth Sci.*, (in press).

Sorokin, A.A., Kotov, A.B., Salnikova, E.B., et al., First data on the age of Early Paleozoic granitoids from the Malyi Khingan terrane of the Central Asian Fold Belt, *Dokl. Earth Sci.*, 2010a, vol. 431, no. 1, pp. 299–303.

Sorokin, A.A., Kotov, A.B., Salnikova, E.B., et al., Granitoids of the Tyrma-Bureya Complex in the northern Bureya-Jiamusi superterrane of the Central Asian Fold Belt: age and geodynamic setting, *Russ. Geol. Geophys.*, 2010b, vol. 51, no. 5, pp. 563–571.

Sorokin, A.A., Kotov, A.B., Sal'nikova, E.B., et al., Early Paleozoic granitoids in the Lesser Khingan terrane, Central Asian Foldbelt: Age, geochemistry, and geodynamic interpretations, *Petrology*, 2011, vol. 19, no. 6, pp. 601–617.

Sorokin, A.A., Smirnova, Yu.N., Kotov, A.B., et al., Sources of Paleozoic terrigenous rocks from the Oldoi terrane of the Central Asian Fold Belt inferred from isotopic-geochemical (Sm-Nd) and geochronological (U-Pb, LA-ICP-MS) data, *Dokl. Earth Sci.*, 2012, vol. 445, no. 2, pp. 969–972.

Sorokin, A.A. and Kudryashov, N.M., Early Mesozoic magmatism of the Bureinskii terrane of the Central Asian Foldbelt: age and geodynamic setting, *Dokl. Earth Sci.*, 2013, vol. 452, no. 1, pp. 915–921.

Sorokin, A.A., Smirnova, Yu.N., Kotov, A.B., et al., Provenances of the paleozoic terrigenous sequences of the Oldoi terrane of the Central Asian Orogenic Belt: Sm-Nd isotope geochemistry and U-Pb geochronology (LA-ICP-MS), *Geochem. Int.*, 2015, vol. 53, no. 6, pp. 534–544.

Sorokin, A.A., Kotov, A.B., Smirnova, Yu.N., et al., On the age of terrigenous deposits of the Khingan Group of the Lesser Khingan terrane (the eastern part of the Central Asian Fold Belt), *Dokl. Earth Sci.,* (in press).

Taylor, S.R. and McLennan, S.M., *The Continental Crust: its Composition and Evolution*, Blackwell: Sci. Publ., 1985.

Visser, J.N.J. and Young, G.M., Major element geochemistry and paleoclimatology of the Permo–Carboniferous glaciogene Dwyka Formation and post-glacial mudrocks in Southern Africa, *Palaeogeogr., Palaeoclim., Palaeoecol.*, 1990, vol. 81, pp. 49–57.

Whitehouse, M.J., Kamber, B.S., and Moorbath, S., Age significance of U-Th-Pb zircon data from Early Archaean rocks of west Greenland—a reassessment based on combined ion-microprobe and imaging studies, *Chem. Geol.*, 1999, vol. 160, pp. 201–224.

Wilde, S.A., Zhang, X.Z., and Wu, F.Y., Extension of a newly-identified 500 Ma metamorphic terrain in northeast China: further U-Pb SHRIMP dating of the Mashan complex, Heilongjiang Province, China, *Tectonophysics*, 2000, vol. 328, pp. 115–130.

Wilde, S.A., Wu, F.Y., and Zhang, X.Z., Late Pan-African magmatism in northeastern China: SHRIMP U-Pb zircon evidence for igneous ages from the Mashan complex, *Precambrian Res.*, 2003, vol. 122, pp. 311–327.

Winchester, J.A. and Floyd, P.A., Geochemical discrimination of different magma series and their differentiation products using immobile elements, *Chem. Geol.*, 1977, vol. 20, pp. 325–343.

Wu, F.Y., Sun, D.Y., Ge, W.C., et al., Geochronology of the Phanerozoic granitoids in northeastern China, *Asian J. Earth Sci.*, 2011, vol. 41, pp. 1–30.

Yang, H., Ge, W.C., Zhao, G.C., et al., Geochronology and geochemistry of Late Pan-African intrusive rocks in the Jiamusi–Khanka block, NE China: petrogenesis and geodynamic implications, *Lithos*, 2014, vol. 208-209, pp. 220–236.

Yudovich, Ya.E., Dembovskii, B.Ya., and Ketris, M.P., Geochemical signs of redeposition of the Ordovician weathering crust in the Pechora Urals, in *Tr. Inst. geol. Komi filiala Akad. Nauk SSSR "Ezhegodnik-1976"* (Proc. Inst. Geol. Komi Branch Akad. Nauk USSR "Yearbook-1976"), Syktyvkar: Inst. Keol. Komi filiala Akad. Nauk SSSR, 1977, pp. 133–142.

Yudovich, Ya.E., *Regional'naya geokhimiya osadochnykh tolshch* (Regional Geochemistry of Sedimentary Strata), Leningrad: Nauka, 1981 [in Russian].

Zhou, J.B., Wilde, S.A., Zhao, G.C., et al., Was the easternmost segment of the Central Asian Orogenic Belt derived from Gondwana or Siberia: an intriguing dilemma? *J. Geodyn.*, 2010, vol. 50, pp. 300–317.

Zhou, J.B. and Wilde, S.A., The crustal accretion history and tectonic evolution of the NE China segment of the Central Asian Orogenic Belt, *Gondwana Res.*, 2013, vol. 23, pp. 1365–1377.

Translated by D. Voroschuk